University of Nevada, Reno

Manipulating Atoms and Molecules with Frequency Combs

A thesis submitted in partial fulfillment of the
requirements for the degree of Master of Science in
Physics

by

Mahmoud Ahmed

Dr. Andrei Derevianko /Thesis Advisor

August, 2010

Abstract

This thesis discusses decelerating atomic beams using pulse trains, and studies the possibility of cooling atoms or molecules using frequency combs. Using frequency combs in laser cooling of multilevel systems may eliminate the need for multiple laser sources, which are currently required to pump the population between manifolds of energy states. It is shown that a small amount of momentum is transferred to two-level atoms during an interaction with a single weak laser pulse. However, there is a considerable change of the atomic momentum when the atoms interact with a pulse train due to the interference between successive pulses.

Acknowledgments

I am heartily thankful to my supervisor, Andrei Derevianko, whose supervision and support from the preliminary to the concluding level enabled me to finish this thesis and graduate. I would like also to thank my parents and my wife for their continues encouragement.

Table of Contents

List of Figures

Chapter 1

Introduction

1.1 Applications of Cold Atoms

Laser cooling is the process of decelerating atoms and molecules using counter-propagating laser radiation which imparts momentum to the atomic or molecular beams. Deceleration of these beams by radiation pressure can produce ensembles of cold atoms and molecules that have a temperature less than 1 μK [1, 2]. Such cold atomic ensembles are of great interest in many fields of physical research, such as optical, atomic, and nuclear physics.

In optical and atomic physics cold atoms may be found in many applications. For example, they are required in optical frequency standards [3, 4], which are devices for producing or probing frequencies. Also, they play a key role in super-high resolution spectroscopy [5, 6], atomic clocks [7], as well as cold and ultra cold collisions [8, 9]. Besides these uses, cold atoms paved the way to the first experimental realization of Bose-Einstein condensation (BEC) [10, 11].

Along with their applications in atomic and optical physics, cold atoms can also be found in the field of nuclear and particle physics. The possibility to cool and trap significant quantities of short-lived radioactive atoms with laser light enabled the study

of radioactive decay of isotopes such as ^{21}Na [12]. Furthermore, the technique of laser cooling and trapping of isotopes has improved trace analysis methods dramatically. For example, it has been used to count individual krypton-85 and krypton-81 atoms present in a natural krypton gas sample with isotopic abundances in the range of 10^{-11} and 10^{-13}, respectively [13].

1.2 Overview of Some Laser Cooling Experiments

The possibility of trapping neutral atoms near the nodes or antinodes of a standing wave was first suggested by Letokhov in 1968 [14]. A few years later, Kazantsev predicted the existence of velocity-dependent forces acting upon an atom moving in an intense standing wave [15].

The concept of radiation-pressure cooling of atoms was suggested in 1975 by Hänsch and Schawlow [16]. They showed that light exerts a radiation pressure on any substance which reflects or scatters it. Thus, a low-density gas can be cooled by illuminating it with intense, quasi-monochromatic light confined to the lower-frequency half of a resonance line's Doppler width. Three years later, the first observation of radiation-pressure cooling on a system by Walls *et al.* was reported [17]. They were able to cool Mg II ions to less than 40 K by irradiating them with $8-\mu$W dye laser. Additionally, they indicated the possibilty to cool the atoms to 10^{-3} K.

Throughout the 1980s, important experiments on laser cooling were performed. In 1982 Phillips and Metcalf built the first Zeeman slower, as a solution to the problems of the Doppler shift and the optical pumping [18]. The problem of the Doppler shift is while the Na atoms slow down in the experiment, they experience Doppler shift out of resonance. The other problem is when the Na atoms are excited from one of the two hyperfine levels in the ground states $3S$ to the $3P$ excited state, the excited atoms may decay to the other hyperfine ground state. Phillips and Metcalf were able

to solve theses problems by using a spatially varying magnetic field applied along the laser atomic beam axis. They demonstrated in their experiment that the magnetic field can Zeeman tune the decelerating atoms into constant resonance with the fixed frequency cooling laser. Also, the applied field is capable of producing selection rules and Zeeman shifts that strongly discriminate against optical pumping.

In 1985, Chu *et al.* [19] experimentally demonstrated the idea of the "optical molasses." They were able to confine the atoms in a small region in space for times of the order ~ 0.1 sec, and cool them to ~ 240 μK. The basic scheme was not a trap but rather a confinement, and they proposed the configuration to be as follows. An atom moving with velocity $+v_x$ will blue shift into resonance with a red detuned laser beam propagating towards $-\hat{x}$. Thus, with the use of six beams along $\pm\hat{x}$, $\pm\hat{y}$, and $\pm\hat{z}$, and averaging over many absorptions, the net effect is a viscous damping force opposite the velocity of the atom.

Another milestone was reached in 1987. Raab *et al.* [20] introduced the first magneto-optical trap (MOT), which relies on near-resonance radiation pressure to both confine and cool the atoms. In a MOT, atoms can be trapped using six red detuned, circularly polarized, counter-propagating laser beams together with a quadruple magnetic field. The magnetic field is created by two coils carrying opposite currents, which produce zero field in the middle and change linearly along x, y, and z axes. If the circular polarization of the lasers are set correctly, a linear restoring force is produced in each direction. This apparatus managed to trap as many as 10^7 atoms for 2 minutes. Once the atoms were trapped, they were cooled to less than a millikelvin and compacted into a region less than 0.5 mm in diameter.

The preceding paragraphs have outlined Doppler cooling, the most common method of laser cooling, on which this thesis is based. However, there are several similar processes that are also referred to as laser cooling, in which photons are used to pump

heat away from a material and thus cool it. These are sisyphus cooling [21], resolved sideband cooling [22],and cavity mediated cooling [23].

1.3 Cooling Atoms Using Pulses

In the preceding section we have presented a brief history on laser cooling using continuous wave (CW) lasers. Here we will summarize some previous works on cooling atoms using pulses.

In 1992 Mark Kasevich and Steven Chu demonstrated the ability to cool sodium atoms in one dimension to an effective temperature of 100 nK for the first time [24]. In their scheme, an atom with two ground states $|1\rangle$ and $|2\rangle$, and one excited state $|e\rangle$, is irradiated by a pulse of light from two laser sources where the first beam at frequency ω_1 and the second beam at frequency ω_2 propagates in opposite direction.

When $\omega_1 - \omega_2$ is nearly equal to the frequency of the $|1\rangle \rightarrow |2\rangle$ transition, these states will behave as a two-level system coupled by a two-photon Raman process[1] [25]. Thus, when the frequency difference $\omega_1 - \omega_2$ is red-detuned from the two photon resonance, an atom moving with velocity $+v$ will Doppler shift the transition into resonance. Consequently, It will receive a momentum kick towards $v = 0$ as it makes the transition $\omega_1 - \omega_2$. Therefore, using sequences of Raman pulses will excite all the atoms except those with a velocity near $v = 0$. Cooling is achieved by following the stimulated excitation with a a pulse of frequency tuned to the $|2\rangle \rightarrow |e\rangle$.

A new approached was introduced in 1995 by Reichel *et al.* which was inspired by Lèvy Flight Statistics to optimize the Raman cooling [26]. In this experiment Reichel

---

[1] Raman cooling is based on two-photon stimulated Raman transitions induced by two laser beams between two states, involving the presence of allowed dipole transitions to a third common state. This leads in effect to a two level description analogous to having a single photon and two level system with wave properties $\mathbf{k} \leftrightarrow \mathbf{k}_1 - \mathbf{k}_2$ and $\omega \leftrightarrow \omega_1 - \omega_2$.

and his colleagues used square pulses in a one dimensional problem with cesium atoms obtaining temperatures below 3 nk.

The last experiment we mention here was done in 2006. Although the lowest temperature achieved in this experiment was not even below 1 K, the method was successfull in cooling very hot atoms ($\sim$ 4000 m/s) [27]. Blinov *et al.* demonstrated broadband laser cooling of atomic ions in an rf trap using ultrafast pulses from a mode-locked laser. They assumed that once the atom was excited, it decays back to the ground state faster than the time period of the mode-locked pulse train T_{rep}. In this case, the atom has little memory between pulses or, equivalently, the absorption spectrum is a single broad line of width $\Delta \sim 1/\tau$ (τ is the pulse duration) and the frequency comb of spacing $1/T_{rep}$ has very little contrast.

The motivation beyond this work relies on the idea that frequency combs, generated by the interference of ultrashort laser pulses, may eliminate the need for multiple laser sources currently needed to achieve efficient cooling.

1.4 Thesis Structure

This introduction provides the foundation for the calculations presented in this thesis. The remainder is as follows. In Chapter 2 an overview is given of the relevant concepts and characteristics of pulse trains and optical frequency combs, which will be used to drive the atoms.

Chapter 3 provides the derivation of the basic equations used in calculating the the probability amplitudes of the atomic states using the Schrödinger equation, together with a brief description of the conditions for complete population inversion and resonance.

In Chapter 4 the density matrix method to find the population in the atomic states is introduced. Also, Chapter 4 provides a brief discussion about laser cooling

of atomic beams and the radiation force when atoms interact with laser pulses. The expressions formulated in Chapter 4 set the foundation for the two following chapters.

In Chapter 5 we present the results of simulations for the Doppler cooling of a two-level system with a single laser pulse. This Chapter shows a comparison between the results of the numerical calculations and the analytical approach for the coherences and the momentum imparted to the atoms after the interaction.

Chapter 6 extends the calculations in Chapter 5 to the cooling with pulse train (frequency comb). It contains a detailed discussion about population transfer due to coherent interaction and the momentum imparted to the atoms through the interaction.

The thesis also includes several appendices containing relevant supplementary information. The Fortran code used to calculate the numerical results presented in Chapter 5 and 6 is included in Appendix D.

Chapter 2

Frequency Combs

2.1 Introduction

Experiments on the excitation of atoms and molecules using frequency combs have become a major interest. Frequency combs are generated by an interference of ultrashort pulses in a train. The selective excitation of the population in the molecular vibrational levels is required for many applications such as quantum computing [28, 29], ultrahigh resolution spectroscopy [30], and chemical reactions [31].

An optical frequency comb is an electromagnetic field that contains a set of regularly-spaced frequencies $f_m = f_0 + mf_{rep}$, where $m = 0 \pm 1 + \pm 2 + ...$ f_{rep} is the frequency interval and f_0 is the offset from zero [32]. The frequency spectrum is related to a train of successive short pulses in the time domain by the Fourier transform; the spacing between the comb frequencies is related to the time interval between pulses T_{rep} by $f_{rep} = 1/T_{rep}$. The width of each tooth of the comb is $1/NT_{rep}$, where N is the number of pulses in the train which contributes to the interference; therefore, for large N the comb teeth will be extremely narrow. Using a train of femtosecond laser pulses to generate a frequency comb as a driving field will keep us away from the obstacles introduced by the excitation of the atomic and molecular

energy levels using single pulses. These obstacles are: the multilevel excitation of the excited vibrational levels caused by the broad spectrum of a femtosecond pulse, and the inefficient interaction between the weak pulse and the atom or the molecule [33].

Consider a truncated train of N laser pulses $f(t)$ as depicted in Fig.(2.1), that is used to excite the atoms or the molecules. The train has the profile

$$f(t) = \sum_{n=0}^{N-1} \mathrm{g}(t - nT_{rep})e^{in\phi},$$

where $\mathrm{g}(t - nT_{rep})$ is the envelope of the pulses, and ϕ is the phase difference between two consecutive pulses. The pulses are identical, have a fixed repetition period T_{rep}. The electric field profile of the train in the time domain is then

$$\begin{aligned}
\boldsymbol{\mathcal{E}}(z,t) =& \frac{1}{2}\hat{\epsilon}\mathcal{E}_0 f(t)e^{i(k_L z - \omega_L t)} + c.c., \\
\boldsymbol{\mathcal{E}}(z,t) =& \frac{1}{2}\hat{\epsilon}\mathcal{E}_0 \sum_{n=0}^{N-1} \mathrm{g}(t - nT_{rep})e^{in\phi}e^{i(k_L z - \omega_L t)} + c.c..
\end{aligned} \tag{2.1}$$

Here $\mathcal{E}_0$ is the pulse amplitude which is complex in general, though its complex phase can just be associated with a time delay. Such a time delay has no physical significance for the problem at hand, and thus $\mathcal{E}_0$ will be assumed real [34]. $k_L = \omega_L/c$ is the wave vector, ω_L is the carrier or the laser frequency, and c.c. stands for the complex conjugate of the preceding term. Here $\hat{\epsilon}$ is the polarization vector and $\hat{\epsilon} \cdot \mathbf{k}_L = 0$.

The detailed derivation for the Fourier transform of the pulse train (2.1) is included in Appendix A. The Fourier transform of the electric field is given by Eq.(A.5)

$$\mathcal{E}(\omega) = [F_1^+(\omega)\frac{\sin\left(\frac{N}{2}\zeta T_{rep}\right)}{\sin\left(\frac{1}{2}\zeta T_{rep}\right)} + F_1^-(\omega)\frac{\sin\left(\frac{N}{2}\eta T_{rep}\right)}{\sin\left(\frac{1}{2}\eta T_{rep}\right)}]. \tag{2.2}$$

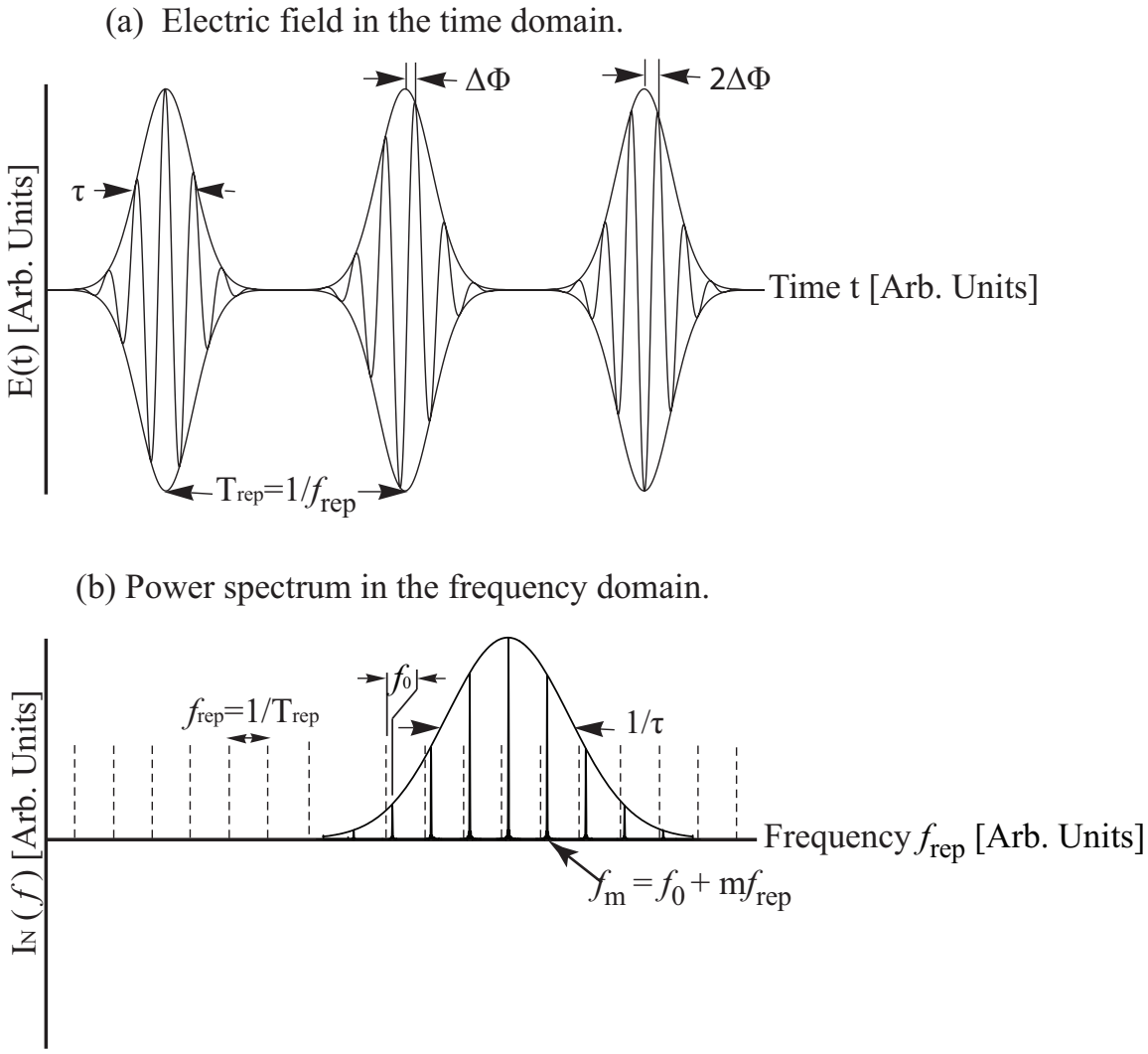

Figure 2.1: (a) A train of Gaussian pulses in the time domain showing the real electric field (in arbitrary units) and the envelope as a function of the time (in arbitrary units). (b) The Fourier transform of the pulse train (frequency domain picture).

where

$$\zeta = (\omega - \omega_L) + \frac{\phi}{T_{rep}},$$
$$\eta = (\omega + \omega_L) - \frac{\phi}{T_{rep}}.$$

Also, $F_1^+(\omega)$ is the Fourier transform of the first pulse and $F_1^-(\omega)$ is the Fourier transform of its complex conjugate.

Eq.(2.2) has the behavior shown in Fig.(2.2). When the arguments of the numerator sin functions (i.e. $N\zeta T_{rep}/2$ or $N\eta T_{rep}/2$) become an integer multiple of π, the numerator vanishes and the fraction gives zero. However, when the sin functions in a numerator and its denominator become zero simultaneously, the fraction will not vanish, but instead it will give a peak of magnitude proportional N.

2.2 Power Spectrum of the Frequency Comb

The energy associated with a harmonic wave is proportional to the amplitude squared. And since the Fourier transform tells us the amplitudes of all the constituent frequencies that make up the input signal, the square of the transform provides a measure of the distribution of energy, or power, at each and every component frequency. Consequently, the square of the transform is a function of frequencies called the power spectrum.

Here we study the behavior of the first term on the r.h.s of Eq.(2.2) by using the L'Hôpital rule (this study is applicable also to the second term). From the L'Hôpital rule

$$\lim_{\zeta T_{rep}\to 0} \frac{\sin\left(\frac{N}{2}\zeta T_{rep}\right)}{\sin\left(\frac{1}{2}\zeta T_{rep}\right)} = N\frac{\cos\left(\frac{N}{2}\zeta T_{rep}\right)}{\cos\left(\frac{1}{2}\zeta T_{rep}\right)},$$

therefore, we have two special cases:

- When $\zeta = 2m\pi/T_{rep}$ the spectral density increases by the factor of N.
- When $\zeta \neq 2m\pi/T_{rep}$ the spectral density becomes zero.

Here $m = 0, \pm1, \pm2, \cdots$,etc. The power spectrum $I_N(\omega)$ for N pulses can now be calculated from

$$I_N(\omega) \propto |\mathcal{E}(\omega)|^2 \propto N^2 \frac{\cos^2(\frac{N}{2}\zeta T_{rep})}{\cos^2(\frac{1}{2}\zeta T_{rep})}.$$

The preceding equation states that the peaks occurs when both the numerator and the denominator simultaneously are zeros.

2.3 Frequency Comb Parameters

In this section we will find two characteristic expressions for the frequency comb, one is the frequency separation between the teeth, and the other is the width of a single tooth.

The teeth separation is simply the frequency separation between any two successive zeros of the denominator of Eq.(2.2), i.e.,

$$\sin(\frac{1}{2}\zeta T_{rep}) = 0.$$

From the definition of ζ, this translates into

$$\frac{1}{2}((\omega_n - \omega_L)T_{rep} + \phi) = n\pi. \tag{2.3}$$

Therefore, the teeth separation in the frequency domain between any two teeth ω_n and ω_{n+1} reads

$$\omega_{rep} = \omega_{n+1} - \omega_n = \frac{2\pi}{T_{rep}}.$$

This equation states that the value of the phase does not affect the teeth separation.

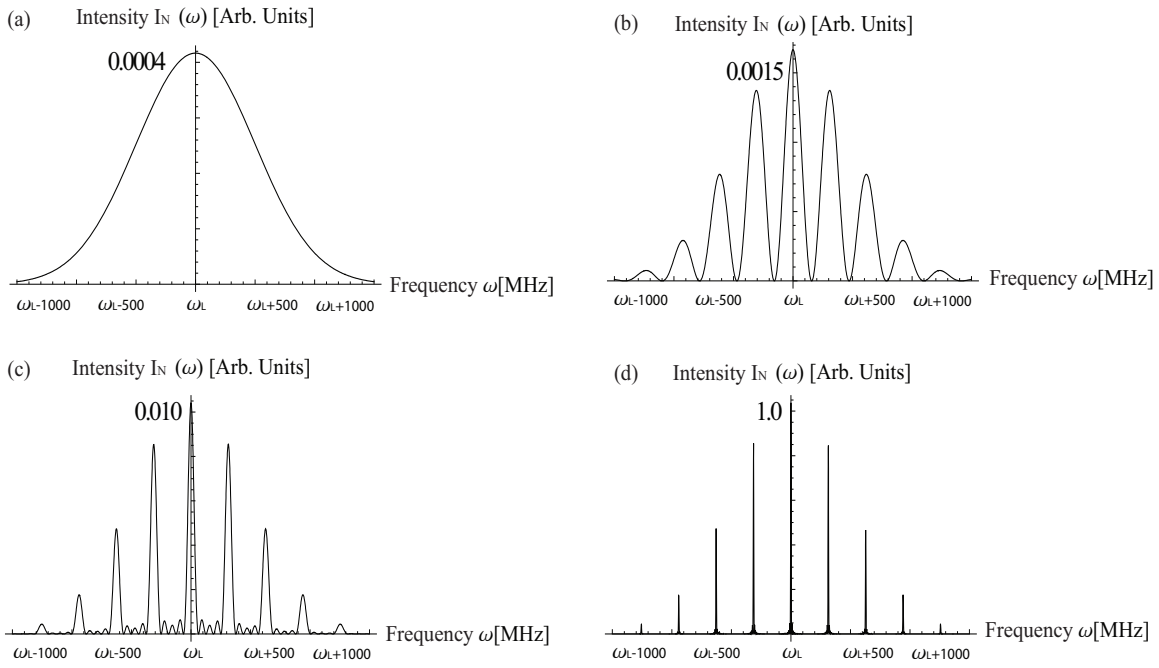

Figure 2.2: The interference pattern in the frequency domain of a train of Gaussian pulses with a repetition period $T_{rep} = 4$ ns in the time domain. The frequency comb envelope is centered around the laser carrier frequency ω_L as the phase shift between the pulses is zero. The number of train pulses affects the width of the individual teeth rather than the number of teeth in the comb. The intensity of the teeth in the frequency comb is progressively proportional to the square of the number of pulses. The number of pulses is (a)$N = 1$, (b)$N = 2$, (c)$N = 5$ and (d)$N = 50$.

The phase, however, shifts the whole comb structure around the carrier frequency ω_L depending on its value as shown in Fig.(2.3).

The phase-dependence of the frequency comb shift could be inferred from Eq.(2.3). For the first tooth $n = 1$, the shift is

$$\omega_{shift} = \omega_1 - \omega_L = \frac{2\pi}{T_{rep}} - \frac{\phi}{T_{rep}}.$$

The last equation confirms that the values of $\phi = 0$ and $\phi = 2\pi$ are identical since it is a property of periodic functions. This means that for the value of $\phi = 2\pi$ the positions of the teeth in the comb are identical to those positions for the case of $\phi = 0$. The maximum shift in the teeth positions in the frequency comb is $\omega_{rep}/2$, as plotted

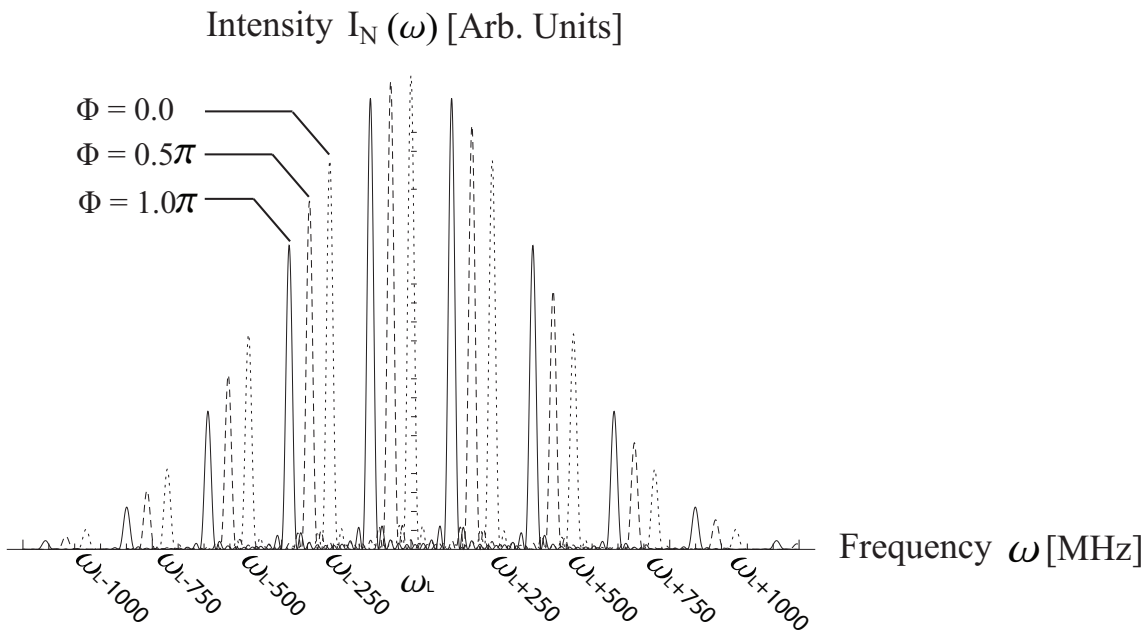

Figure 2.3: Dependence of the comb teeth positions in the frequency domain on the phase between the pulses in the time domain. The tooth separation is 250 MHz corresponding to a repetition period in the time domain $T_{rep} = 4$ ns. When $\phi = 0, \phi = 2\pi$ the comb is centered inside the Gaussian envelope and there will be a tooth at the carrier frequency ω_L. but as the phase begins to increase the comb teeth move to the left to a maximum shift of $\omega_{rep}/2$, which corresponds to phase a $\phi = \pi$.

in Fig.(2.3) which corresponds to the value of $\phi = \pi$.

Derivation of a single tooth width is similar to the previous procedure but using the sin functions in the numerator instead of the denominator. In Eq.(2.2) the argument of the numerator is N times the argumaent of the denominator, therefore, the oscillation of the numerator sinusoidal function is fast compared to the denominator. Thus, the magnitude of the numerator will decline very fast to zero, while that of the denominator is still appreciable. Consequently, a tooth requires two oscillations. One oscillation to bring the magnitude from zero to a maximum, then another oscillation to bring the intensity to zero again.

The zeros of the sin function in the numerator of Eq.(2.2) occur when

$$\frac{N}{2}((\omega_n - \omega_L)T_{rep} + \phi) = n\pi,$$

the tooth width is

$$\Delta\omega_{width} = \omega_{n+2} - \omega_n = \frac{4\pi}{NT_{rep}},$$

and

$$\Delta\omega_{FWHM} \approx \frac{2\pi}{NT_{rep}}.$$

This is the full angular frequency width of a single tooth in the frequency comb at half maximum.

2.4 The Interference picture of Infinite Number of Pulses

As $N \to \infty$, the peaks in the frequency comb get progressively higher and proportionately narrower, so that they ultimately approach Dirac delta functions. From Eq.(2.2), the term responsible for the comb structure is

$$\lim_{N\to\infty} \frac{\sin(\frac{N}{2}\zeta T_{rep})}{\sin(\frac{1}{2}\zeta T_{rep})} = \frac{2\pi}{T_{rep}} \sum_m \delta(\zeta - \frac{2m\pi}{T_{rep}}). \tag{2.4}$$

The substitution of Eq.(2.4) into Eq.(2.2) gives the frequency comb spectrum represented by an infinite sum of delta functions as

$$\mathcal{E}(\omega) = \frac{2\pi}{T_{rep}}[F_1^+(\omega) \sum_m \delta(\zeta - \frac{2m\pi}{T_{rep}}) + F_1^-(\omega) \sum_n \delta(\eta - \frac{2n\pi}{T_{rep}})].$$

Applying the inverse Fourier transform to the preceding equation gives

$$\boldsymbol{\mathcal{E}}(t) = \sqrt{\frac{\pi}{2}}\frac{\tau}{T_{rep}}\mathcal{E}_0[\sum_m e^{-\frac{\tau^2(-2m\pi+\phi)^2}{2T_{rep}^2}} \cdot e^{i(-\frac{\phi}{T_{rep}}+m\omega_{rep}+\omega_L)t} + \sum_n e^{-\frac{\tau^2(2n\pi+\phi)^2}{2T_{rep}^2}} \cdot e^{i(\frac{\phi}{T_{rep}}+n\omega_{rep}-\omega_L)t}]. \quad (2.5)$$

It can be inferred from the last equation that when an atom is irradiated by a train of Gaussian pulses, the atom will be effectively subjected to a large number of laser sources with frequencies separated by $\omega_{rep} = 2\pi/T_{rep}$. The first exponential function is independent of time and frequency; it just acts as a scaling factor for the amplitudes $\mathcal{E}_0$ for these effective laser sources in the time domain.

Chapter 3

Probability Amplitude Equations for a Multilevel System

3.1 Introduction

Consider driving transitions between initial and final stationary states, $|g, j\rangle$ and $|e, n\rangle$ of a model system as in Fig.(3.1). The two manifolds are separated by an energy gaps $E_{nj} = \hbar(\omega_{en} - \omega_{gj})$ and are connected by a time dependent interaction. Furthermore, no direct interaction is allowed within each manifold.

The driving field is a train of femtosecond Gaussian pulses that interfere to excite many transitions simultaneously. The presence of the external field is required for stimulated absorption and stimulated emission, without which all matrix elements of the perturbing Hamiltonian vanish [35]. In this derivation we will neglect the spontaneous decay of the excited atoms.

To obtain the transition probability amplitudes of the energy levels, when atoms interact with electromagnetic radiation, it is necessary to specify the proper form of the interaction Hamiltonian $\hat{\mathcal{H}}_{int}(\xi, \mathbf{r}, t)$. The interaction Hamiltonian is a function of the set of coordinates ξ that describe the internal atomic motion and the spatial

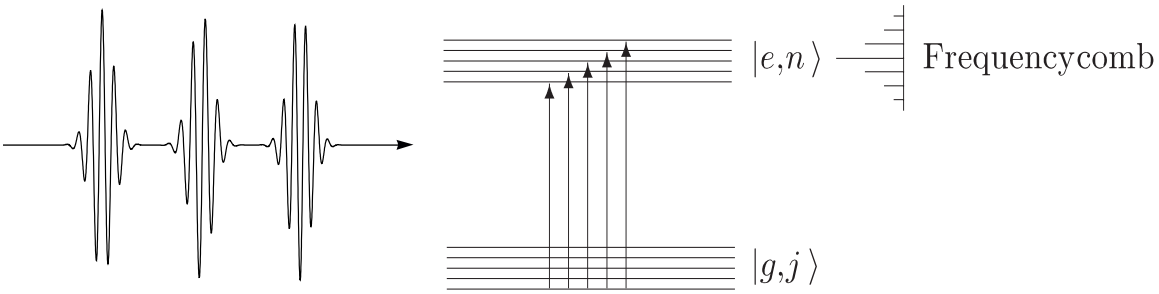

Figure 3.1: Model system to be interacted with a pulse train. States within the ground manifold g are labeled by the quantum number j; and states within the excited manifold e are labeled by the quantum number n. The electric field is assumed to resonant with a g→ e transition.

coordinates **r** that describe the motion of the center of mass of an atom. This electromagnetic field consists of time-varying electric and magnetic fields. Therefore, the time-dependent Hamiltonian that represents the interaction of an atom with the field to leading order is

$$\hat{\mathcal{H}}_{int}(\xi, \mathbf{r}, t) = -\hat{D}(\xi) \cdot \boldsymbol{\mathcal{E}}(\mathbf{r}, t), \tag{3.1}$$

where $\hat{D}(\xi)$ is the dipole matrix operator, and $\boldsymbol{\mathcal{E}}(\mathbf{r}, t)$ is the time-dependent electric field. This dipole-electric interaction is the dominant term, as the coupling to magnetic field is much smaller in magnitude[1].

We use Schrödinger equation to find the probability amplitudes of the energy states and the equations that govern their time evolution. We start by writing the state of our model system in the interaction picture [36] at some arbitrary time t in

[1]In the interaction Hamiltonian equation, we neglected the term $-(e/m)\hat{S} \cdot \boldsymbol{\mathcal{B}}(\mathbf{r}, t)$, which is the interaction of the spin magnetic moment of the electron with the oscillating magnetic field of the plane wave. The relative order of magnitude of the spin-magnetic field interaction term to the dipole-electric interaction term $\simeq a_0/\lambda \ll 1$. Usually, λ is much greater than a_0, the Bohr radius.

terms of the unperturbed eigenstates as

$$|\Psi\rangle = \sum_{j=0}^{v_a} a_j(t) e^{-i\omega_{gj}t}|g,j\rangle + \sum_{n=0}^{v_b} b_n(t) e^{-i\omega_{en}t}|e,n\rangle, \tag{3.2}$$

where $a_j(t)$ and $b_n(t)$ are the probability amplitudes of the ground eigenstates j or the excited eigenstates n respectively. v_a and v_b are the numbers of states in the ground and excited manifolds respectively. We assume that if $t = t_0$, then $b_n(t) = 0$ and $a_j(t) = \delta_{j0}$, where δ_{j0} is the Dirac delta function. Thus, all the population is initially in the ground state. The equations of motion governing the time evolution of the probability amplitudes $a_j(t)$ and $b_n(t)$ are derived from the Schrödinger equation

$$i\hbar\frac{\partial}{\partial t}|\Psi\rangle = \hat{\mathcal{H}}|\Psi\rangle. \tag{3.3}$$

The Hamiltonian describing the interaction of such an atom with the external classical electric field can be written as

$$\hat{\mathcal{H}} = \hbar(\sum_{j=0}^{v_a} \omega_{gj}|g,j\rangle\langle j,g| + \sum_{n=0}^{v_b} \omega_{en}|e,n\rangle\langle n,e|) - \hat{D}(\xi)\cdot\boldsymbol{\mathcal{E}}(\mathbf{r},t). \tag{3.4}$$

In Eq.(3.4), the first term on the r.h.s corresponds to the Hamiltonian that governs the field-free evolution of the system. The second term is the interaction Hamiltonian that drives the dipole transitions excited by the electric field. Such a Hamiltonian model for wave packet excitation is very common in the literature [35–37].

In the long-wavelength approximation[2], the classical electric field may be replaced

---

[2]For atomic systems, the relevant length scale for the particles is approximately determined by the atomic Bohr radius ($a_0 = 0.5$ $\mathring{A}$), which is typically four orders of magnitude smaller than the optical wavelengths that determine the characteristic length scale of the optical fields. Therefore, in the long-wavelength approximation $\mathbf{k}\cdot\mathbf{r} \to 0$, and $e^{-i\mathbf{k}\cdot\mathbf{r}} \approx 1$.

by its value at $r = 0$

$$\boldsymbol{\mathcal{E}}(\mathbf{r},t) \approx \boldsymbol{\mathcal{E}}(t) = \frac{1}{2}\hat{\epsilon}\mathcal{E}_0 f(t) e^{-i\omega_L t} + c.c.$$

On substituting Eq.(3.2) of the wave function expansion into the Schrödinger Eq.(3.3), we find the coupled differential equations for the probability amplitudes. The l.h.s. of resulting equation is

$$\begin{aligned} i\hbar\frac{\partial}{\partial t}|\Psi\rangle =& i\hbar\sum_{j=0}^{v_a}\dot{a}_j(t)e^{-i\omega_{gj}t}|g,j\rangle + \hbar\omega_{gj}\sum_{j=0}^{v_a}a_j(t)e^{-i\omega_{gj}t}|g,j\rangle \\ &+ i\hbar\sum_{n=0}^{v_b}\dot{b}_n(t)e^{-i\omega_{en}t}|e,n\rangle + \hbar\omega_{en}\sum_{n=0}^{v_b}b_n(t)e^{-i\omega_{en}t}|e,n\rangle, \end{aligned} \tag{3.5}$$

while the r.h.s. is

$$\begin{aligned} \hat{\mathcal{H}}|\Psi\rangle =& \hbar(\sum_{j=0}^{v_a}\omega_{gj}|g,j\rangle\langle j,g|\sum_{j=0}^{v_a}a_j(t)e^{-i\omega_{gj}t}|g,j\rangle) \\ &+ \sum_{n=0}^{v_b}\omega_{en}|e,n\rangle\langle n,e|\sum_{j=0}^{v_a}a_j(t)e^{-i\omega_{gj}t}|g,j\rangle \\ &+ \sum_{j=0}^{v_a}\omega_{gj}|g,j\rangle\langle j,g|\sum_{n=0}^{v_b}b_n(t)e^{-i\omega_{en}t}|e,n\rangle \\ &+ \sum_{n=0}^{v_b}\omega_{en}|e,n\rangle\langle n,e|\sum_{n=0}^{v_b}b_n(t)e^{-i\omega_{en}t}|e,n\rangle \\ &- \frac{1}{2}(\hat{D}\cdot\hat{\epsilon})\mathcal{E}_0 f(t)e^{-i\omega_L t}\sum_{j=0}^{v_a}a_j(t)e^{-i\omega_{gj}t}|g,j\rangle \\ &- \frac{1}{2}(\hat{D}\cdot\hat{\epsilon})\mathcal{E}_0 f(t)e^{-i\omega_L t}\sum_{n=0}^{v_b}b_n(t)e^{-i\omega_{en}t}|e,n\rangle \\ &- \frac{1}{2}(\hat{D}\cdot\hat{\epsilon})\mathcal{E}_0 f(t)^* e^{+i\omega_L t}\sum_{j=0}^{v_a}a_j(t)e^{-i\omega_{gj}t}|g,j\rangle \\ &- \frac{1}{2}(\hat{D}\cdot\hat{\epsilon})\mathcal{E}_0 f(t)^* e^{+i\omega_L t}\sum_{n=0}^{v_b}b_n(t)e^{-i\omega_{en}t}|e,n\rangle. \end{aligned} \tag{3.6}$$

To determine the probability amplitude $a_j(t)$ of the eigenstates $|g,j\rangle$, we need to multiply the the r.h.s of the last two equations by the bra $\langle g,j|$ and then equate them to each other. Thus, the resulting equation is

$$\begin{aligned} i\hbar\dot{a}_j(t)e^{-i\omega_{gj}t} + \hbar\omega_{gj}a_j(t)e^{-i\omega_{gj}t} =& \hbar\omega_{gj}a_j(t)e^{-i\omega_{gj}t} \\ &- \frac{1}{2}\sum_{n=0}^{v_b}\langle j,g|\hat{D}\cdot\hat{\epsilon}|e,n\rangle f(t)\mathcal{E}_0 e^{-i\omega_L t}b_n(t)e^{-i\omega_{en}t} \\ &- \frac{1}{2}\sum_{n=0}^{v_b}\langle j,g|\hat{D}\cdot\hat{\epsilon}|e,n\rangle f(t)^*\mathcal{E}_0 e^{+i\omega_L t}b_n(t)e^{-i\omega_{en}t}, \end{aligned}$$

or in a compact form

$$\begin{aligned} \dot{a}_j(t) =& \frac{i}{2}\sum_{n=0}^{v_b}\frac{\langle j,g|\hat{D}\cdot\hat{\epsilon}|e,n\rangle\mathcal{E}_0}{\hbar}f(t)b_n(t)e^{-i(\omega_L+\omega_{en}-\omega_{gj})t} \\ &+ \frac{i}{2}\sum_{n=0}^{v_b}\frac{\langle j,g|\hat{D}\cdot\hat{\epsilon}|e,n\rangle\mathcal{E}_0}{\hbar}f(t)^*b_n(t)e^{i(\omega_L-\omega_{en}+\omega_{gj})t}. \end{aligned}$$

Further, near the resonance (when $\omega_L \approx \omega_{en} - \omega_{gj}$), the sinusoidal terms with arguments $(\omega_L + \omega_{en} - \omega_{gj})$ and ω_L vary more rapidly than those of argument $(\omega_L - \omega_{en} + \omega_{gj})$. The former rapidly varying terms do not make significant contributions to the differential equations for long times: they average out. This is referred to as the "rotating wave approximation"[3]. For the rotating wave approximation we retain only terms containing $(\omega_L - \omega_{en} + \omega_{gj})$ in the preceding equation to obtain

$$\dot{a}_j(t) = \frac{i}{2}\sum_{n=0}^{v_b}\frac{\langle j,g|\hat{D}\cdot\hat{\epsilon}|e,n\rangle\mathcal{E}_0}{\hbar}f(t)^*b_n(t)e^{i(\omega_L-\omega_{en}+\omega_{gj})t}. \tag{3.7}$$

The probability of finding the system in one of the eigenstates $|e,n\rangle$ at time t can be derived by following the same procedure as for $a_j(t)$. On multiplying Eq.(3.5) and

---

[3]See Appendix B for detailed discussion of the rotating wave approximation.

Eq.(3.6) from the left by the bra $\langle e, n|$ and equating them to each other, we obtain

$$\dot{b}_n(t) = \frac{i}{2} \sum_{n=0}^{v_b} \frac{\langle j, g|\hat{D} \cdot \hat{\epsilon}|e, n\rangle \mathcal{E}_0}{\hbar} f(t) a_j(t) e^{-i(\omega_L - \omega_{en} + \omega_{gj})t}. \tag{3.8}$$

Eq.(3.8) and Eq.(3.7) give a pair of coupled differential equations for the probability amplitudes $a_j(t)$ and $b_n(t)$ of the two manifolds of the ground state and the excited state as in Fig.(3.1). They are rewritten here in a slightly different notation as

$$\dot{a}_j(t) = \frac{i}{2} \sum_{n=0}^{v_b} \Omega_{jn} f(t)^* b_n(t) e^{i\delta_n t}, \tag{3.9a}$$

$$\dot{b}_n(t) = \frac{i}{2} \sum_{n=0}^{v_b} \Omega_{jn} f(t) a_j(t) e^{-i\delta_n t}. \tag{3.9b}$$

For convenience, the equations have been rewritten in terms of the Rabi frequency[4]

$$\Omega_{jn} = \frac{\langle j, g|\hat{D} \cdot \hat{\epsilon}|e, n\rangle \mathcal{E}_0}{\hbar},$$

and the detuning

$$\delta_n = \omega_L - \omega_{en} + \omega_{gj},$$

the later is the difference between the incident field carrier frequency and the transition frequency. Detuning is a measure of the amount by which the frequency of the applied field is "off-resonance" from the frequency of the target transition.

---

[4]Rabi frequency is a measure of the interaction strength that gives the the rate at which transitions are coherently induced between the two atomic levels. Qualitatively, it is the frequency of the population oscillation.

3.2 The Complete Population Inversion (CPI)

Conditions for a strong interaction, or a resonance, of the applied electric field with the transition frequencies can be inferred form the comb Eq.(2.3). At the resonance, the transition frequency $(\omega_{en} - \omega_{gj})$ must be equal to one of the frequency comb teeth frequencies. To show this, the frequencies of the comb teeth ω_n from the previous section are

$$\omega_n = \omega_L + \frac{2n\pi}{T_{rep}} - \frac{\phi}{T_{rep}},$$

and the condition to be fulfilled at the resonance is $\omega_n = (\omega_{en} - \omega_{gj})$. Subsequently,

$$(\omega_{en} - \omega_{gj}) = \omega_L + \frac{2n\pi}{T_{rep}} - \frac{\phi}{T_{rep}}.$$

On substituting for the detuning $\delta_n = \omega_L - \omega_{en} + \omega_{gj}$, and rearranging the equation, we obtain

$$\phi = \delta_n T_{rep} + 2n\pi. \tag{3.10}$$

This equation is important to our calculations in this thesis as it helps in tuning the frequency comb teeth to a specific resonance. It relates the detuning and the phase, which we can control to get the resonance. For instance, in case of non-zero detuning $\delta_n \neq 0$, we can change the value of the phase to compensate for the detuning to get into resonance.

In Fig.(3.2), the detuning of the laser frequency from the transition frequency is $\sim 0.1\pi$, and all the population at time $t = 0$ is assumed to be in the ground state as shown. The solid curve is the stimulated absorbtion and emission when $\delta_n = 0.1\pi$. It is shown that when the laser frequency is off-resonance with the transition frequency, most of the population ($\backsim$ 75%) remains in the ground state. On calculating the phase which will compensate for the value of the detuning from Eq.(3.10), we were

able to recover the resonance case, showed by the dashed curve.

Consider the weak excitation limit in which the population of the ground state is change by the interaction of the first pulse, but instead needs N pulses to completely transfer the population to the excited state. Since these first few pulses which extends in time from $-\infty$ to t do not change the population in the ground state significantly, we can substitute for $a_0(t) \approx 1$ in Eq.(3.9b) and then integrate to obtain

$$b_n(t) = \frac{i}{2} \sum_{m=0}^{N-1} \int_{-\infty}^{t} \mathrm{g}(t - mT_{rep}) \Omega_{0n} e^{-i\delta_n t} e^{im\phi} dt.$$

This gives the probability amplitudes of the system to be in one of the excited states. As the pulse width is much shorter than the repetition period and the pulses do not overlap, we can extend the upper limit of the integration to infinity. Therefore, for the first pulse, the probability amplitudes of the excited states is

$$b_n(T_{rep}) = \frac{i}{2} \int_{-\infty}^{+\infty} \mathrm{g}(t) \Omega_{0n} e^{-i\delta_n t} dt.$$

The integral $\int_{-\infty}^{+\infty} \mathrm{g}(t) e^{-i\delta_n t} dt$ has the form of the Fourier transform of $\mathrm{g}(t)$ evaluated at frequency $-\delta_n$, and is thus riven by

$$b_n(T_{rep}) = \frac{i}{2} \sqrt{2\pi} \Omega_{0n} \mathcal{F}_1(-\delta_n).$$

After the interaction with the second pulse at $t = 2T_{rep}$, the amplitudes are

$$b_n(2T_{rep}) = \frac{i}{2} \sqrt{2\pi} \Omega_{0n} \mathcal{F}_1(-\delta_n) + \frac{i}{2} \sqrt{2\pi} \Omega_{0n} \mathcal{F}_1(-\delta_n) e^{i(\phi - \delta_n T_{rep})}.$$

This second pulse transfer another wave packet to the excited state which interferes

(a) Ground state probability amplitude.

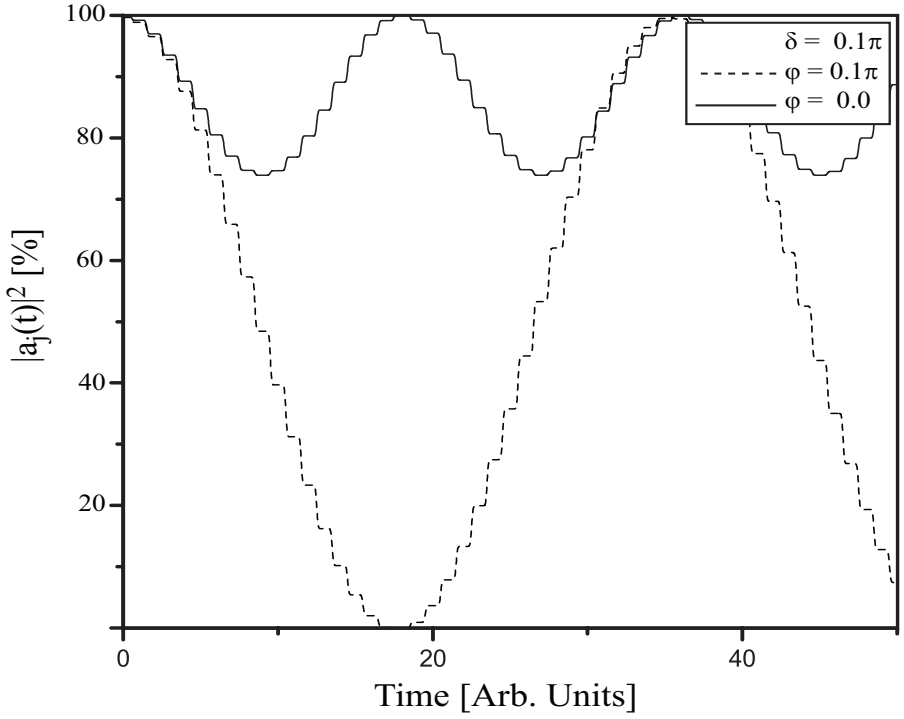

(b) Excited state probability amplitude.

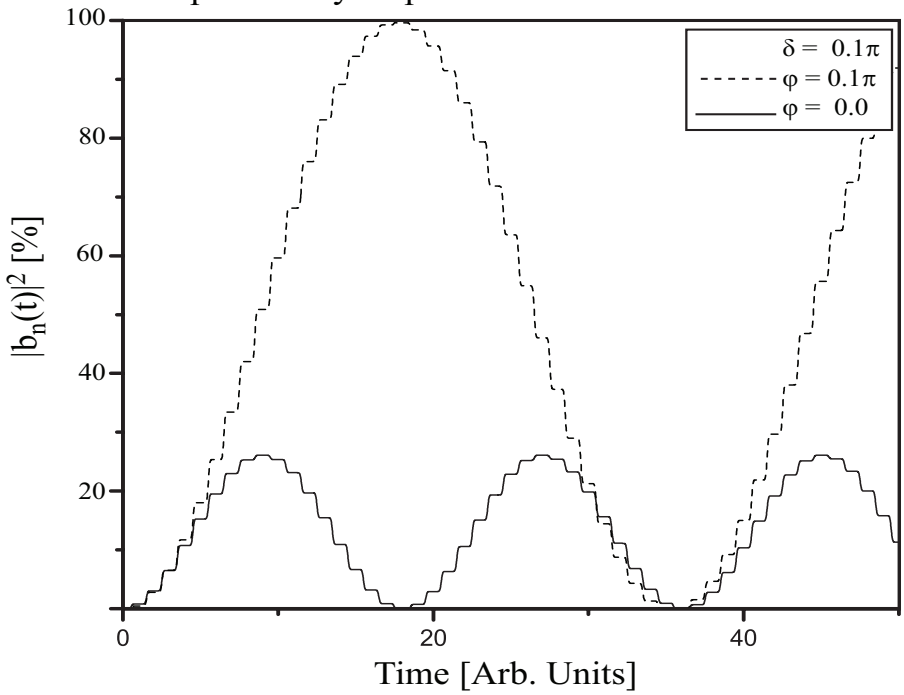

Figure 3.2: A two-level system interacting with laser radiation. Eq.(3.10) holds perfectly as the resonance interaction (dashed curve) is recovered from the off resonance interaction (solid curve).

with the wave packet created by the first pulse [38]. After the excitation by N pulses

$$b_n(NT_{rep}) = \frac{i}{2}\sqrt{2\pi}\Omega_{0n}F_1(-\delta_n)[\sum_{m=0}^{N-1} e^{im(\phi-\delta_n T_{rep})}],$$

and on substituting for the last summation from Eq.(A.4), we obtain

$$b_n(NT_{rep}) = b_n(T_{rep})\frac{\sin(\frac{N}{2}(\phi-\delta_n T_{rep}))}{\sin(\frac{1}{2}(\phi-\delta_n T_{rep}))}.$$

From the previous consideration, in case of zero phase and detuning, the population in the excited state levels increases as the square of the number of pulses and the population accumulated by the first pulse

$$|b_n(NT_{rep})|^2 = N^2|b_n(T_{rep})|^2, \tag{3.11}$$

where we have used the L'Hôpital rule as in the previous section.

As an example, let us consider Fig.(3.2) to illustrate the accumulation dependence. The driving pulses are assumed to have a Gaussian envelope $\mathrm{g}(t) = \exp[-t^2/2\tau^2]$, where $\tau = 0.1$ and $T_{rep} = 1.0$ in arbitrary units. This repetition period is large enough that pulse wings vanish before the next pulse arrives. For a two-level one may define the pulse area

$$\theta = \int_{-\infty}^{\infty} \Omega_{ge}\mathrm{g}(t)dt.$$

If $\theta = \pi$, the atom is driven from the ground state exactly to the excited state, and it is called "$\pi - pulse$" inversion. A "$2\pi - pulse$" takes the atom from the ground state to the excited state then back to the ground state. It is shown in Fig.(3.2) that for our choice of parameters, the pulse area is very small $\theta = \pi/18$ (the dashed line). The first driving pulse merely perturbs the atom, only exciting $\sim 0.78\%$ of the ground state population. After the arrival of the second pulse the the population

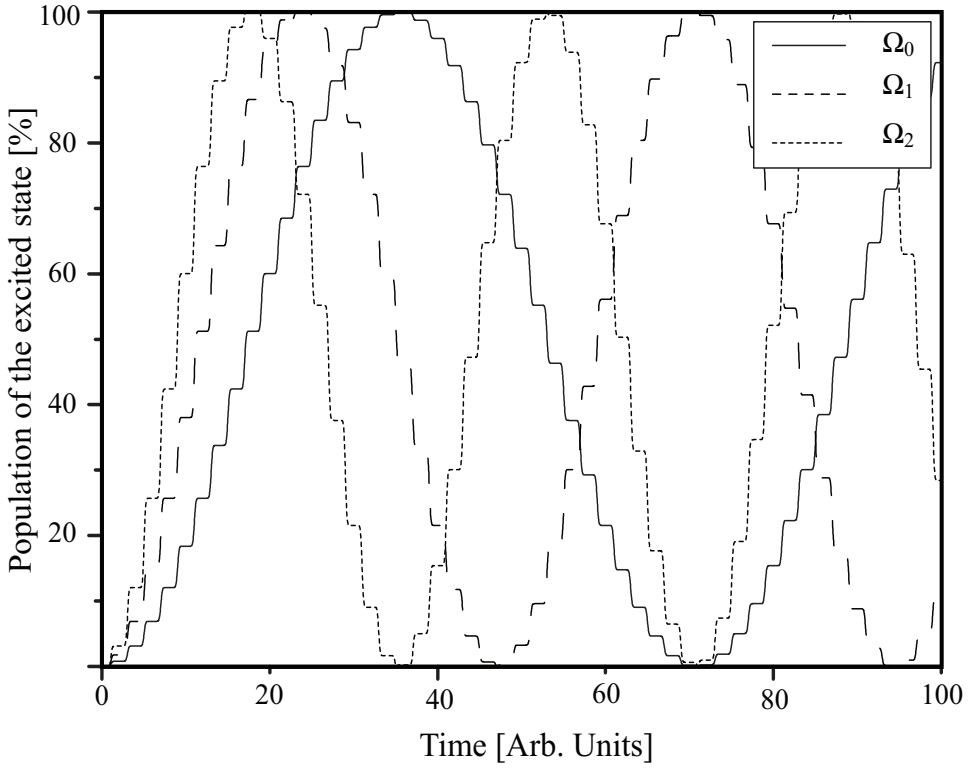

Figure 3.3: The excited state population as a function of time evaluated for different Rabi frequencies. As the Rabi frequency ($\sim \sqrt{I}$) increases, the pulse area will increase and the system needs less number of pulses to reach the complete population inversion. (a) The solid curve is a plot for arbitrary Rabi frequency Ω_0, and the complete population inversion is achieved after 19 pulses, (b) $\Omega_1 = 3\Omega_0/2$, and the complete population inversion is achieved after 16 pulses, and (c) $\Omega_2 = 2\Omega_0$, and the complete population inversion is achieved after 9 pulses.

accumulated in the the excited state is $\sim 3.1\%$. So at the arrival of each new pulse the accumulation increase with the square of the number of pulse as indicated in Eq.(3.11), reaching the CPI after 18 pulses when the total area of the pulses becomes equal to π.

Chapter 4

Manipulating Atoms Using Pulses

4.1 Cooling Atoms Using lasers

The first successful laser cooling of atoms was demonstarted in 1978 by Wineland, Drullinger and Walls [17]. Since then, a variety of techniques have been developed to cool atoms as low as possible. The essence of the laser cooling is based on the fact that photons of a laser beam can impart momentum to the atoms. The simplest technique of laser cooling is the Doppler cooling. It needs only two atomic states and a counterpropagating laser beam tuned near the transition frequency ω_{eg}.

By absorbing a photon, the atom obtains the photon momentum $\hbar \boldsymbol{k}_L$, where $\boldsymbol{k}_L$ is the laser wave vector. The photon momentum $\hbar \boldsymbol{k}_L$ is called the recoil momentum p_{recoil} and is defined as the change in the atomic momentum due to the absorption of a single photon.

After the absorbtion of a photon, we have two possible mechanisms. An atom may spontaneously emit the absorbed photon by decaying from the excited to the ground state, as may emit the photon through a stimulated emission process. If the atom emitted the photon through the spontaneous decay process, there will be a net change in the atomic momentum by an amount of $\Delta p = \hbar \boldsymbol{k}_L$. Although, when the

atom acquires the photon momentum in the process of absorbtion from a specific direction, it will emit the photon in a random direction during spontaneous emission. Therefore, an atom continues to receive impulses in the direction of the laser beam $\boldsymbol{k}_L$, while all the directions in space are equally probable for spontaneous decay, which means $\langle \boldsymbol{k}_s \rangle = 0$, where $\boldsymbol{k}_s$ is the wave vector of the spontaneous emitted photon. The second probable case is that the emission of the photon is stimulated by the laser which originally excited it. In this situation, the direction of the emitted photon will be the same as the absorbed photon. Thus, if an atom got an impulse in a specific direction through the process of absorbtion, the stimulated emitted photon will impart the same momentum to the atom in the opposite direction, resulting in the zero change in the atomic momentum.

As the atoms absorb photons from the laser beam, their velocities will change. One of the important considerations in slowing atomic beams is the effective detuning $\delta_{eff} = \delta - \boldsymbol{k}_L \cdot \boldsymbol{v}_z$, where $\boldsymbol{v}_z$ is the velocity of the atoms in the positive z direction. Atoms in a beam are slowed down by a single laser beam propagating against their direction of motion. Consequenctly, in the frame of reference of the moving atoms, the laser frequency appears higher than the real frequency by an amount of $k_L v_z$, due to the Doppler shift. Detuning below the resonance frequency (δ is negative) is called "red" detuning because the laser frequency is lowered. When the detuning is positive, it is refereed to as "blue" detuning, as the frequency of laser beam is increased.

Atomic temperature is defined from the classical theory of equipartition energy, that is the thermal energy per particle per degree of freedom at a temperature T is given by

$$E = \frac{1}{2} k_B T,$$

where k_B is the Boltzmann constant. In a gas of non-interacting atoms, moving in a single direction, we can set the kinetic energy for a velocity component in this

direction equal to $k_BT/2$ as follows

$$\frac{1}{2}mv_z^2 = \frac{1}{2}k_BT,$$

from which we can find the r.m.s. thermal velocity

$$v_{rms} = \sqrt{\frac{k_BT}{m}}.$$

This equation states that there is a direct relationship between the root mean square of the velocity v_{rms} and the temperature T. We can use this relationship to determine the temperature from measurements of the average speed. It is also the basis of laser cooling, which uses the mechanical force between a laser beam and the moving atoms in a gas to slow them down and hence to produce low temperatures. The temperatures that are now achieved by laser cooling are in the microKelvin range, which corresponds to atomic speeds that are about four orders of magnitude smaller than the velocity at room temperature.

4.2 Cooling Atoms with Laser Pulses

Atoms and molecules mostly are multilevel systems, and their interaction with a radiation field can involve many levels. Nevertheless, if the radiation field frequency ω_L is monochromatic, often we can limit the consideration to the levels which are nearly resonant with that frequency. When only one such excited level exists, a two-level approximation can be made.

Consider a one-dimensional problem of two-level system, moving in the positive z direction, interacting with an electric field in the form of a train of laser pulses traveling in the negative z direction. We will assume that the single pulse intensity

is hardly sufficient to transfer the population from the ground state to the excited state. The total electromagnetic field can be divided into two parts: the classical electromagnetic field exciting the electric dipole transitions of the atom which can be attributed to the first part, and the quantized vacuum field responsible for the spontaneous decay of the atomic state can be considered as the second part of the total field. Thus, the Hamiltonian of the system is given by the sum of the field-free atomic hamiltonian $\hat{\mathcal{H}}_0$ which determines the internal states of the atom, the kinetic energy operator $\hat{\mathbf{P}}^2/2M$ of the center of mass, the interaction Hamiltonian $\hat{\mathcal{H}}_{int}$ for the atom with the laser pulse, the vacuum filed Hamiltonian $\hat{\mathcal{H}}_{vac}$ which determines the quantized vacuum field, and finally $\hat{\mathcal{H}}_\gamma$ which is the operator of the dipole interaction of the atom with the vacuum field that is responsible for the spontaneous emission. Thus, we have

$$\hat{\mathcal{H}} = \hat{\mathcal{H}}_0 + \frac{\hat{\mathbf{P}}^2}{2M} + \hat{\mathcal{H}}_{int} + \hat{\mathcal{H}}_{vac} + \hat{\mathcal{H}}_\gamma. \tag{4.1}$$

The two-level atom Hamiltonian $\hat{\mathcal{H}}_0$ has eigenvalues $\hbar\omega_1$ and $\hbar\omega_2$ for the energies of the ground state and the excited state respectively.

As we are interested in the time evolution of this system after the interaction with laser pulses, we need to consider the "Optical Bloch Equations" derived from the density matrix after considering the relaxation terms. The need for a statistical description via density matrices arises when one considers either an ensemble of systems or one system whose preparation history is uncertain and one does not know with 100% certainty which pure quantum state the system is in [39].

To analyze the problem using the density matrix, we need to specify the interaction Hamiltonian $\hat{\mathcal{H}}_{int}$. From Eq.(3.1) it given by

$$\hat{\mathcal{H}}_{int}(\xi, z, t) = -\hat{D}(\xi) \cdot \boldsymbol{\mathcal{E}}(z, t), \tag{4.2}$$

where $\hat{D}(\xi) = -|e|\xi$ is the dipole moment operator, and $\boldsymbol{\mathcal{E}}(z,t)$ is the space- and time-dependent electric field. The electric field for a train of laser pulses traveling in the negative z direction can be written as

$$\boldsymbol{\mathcal{E}}(z,t) = \frac{\mathcal{E}_0}{2}(f(z,t) + c.c.), \tag{4.3}$$

where

$$f(z,t) = \sum_{n=0}^{N-1} e^{-\frac{(t+\frac{z}{c}-nT_{rep})^2}{2\tau^2}+i(k_L z+\omega_L t)+in\phi},$$

Now we begin working on the problem using the density matrix, which is written as

$$\rho = \begin{pmatrix} \rho_{ee} & \rho_{eg} \\ \rho_{ge} & \rho_{gg} \end{pmatrix} = \begin{pmatrix} b_e b_e^* & b_e a_g^* \\ a_g b_e^* & a_g a_g^* \end{pmatrix},$$

where a_g and b_e are the probability amplitudes of the ground state and the excited state, respectively. The elements of the density matrix have the following interpretation: the diagonal elements ρ_{jj} give the probability that the system is in the eigenstate; the off-diagonal elements ρ_{ji} (or coherences) are non-zero only if the system is in a superposition of energy eigenstate j and i.

The evolution equation for the elements ρ_{ij} may be found from the evolution equation of the amplitudes derived in Chapter 3. For a two-level atom, they have the forms

$$\dot{a}_g(t) = \frac{1}{i\hbar} b_e(t) \hat{\mathcal{H}}_{ge}(\xi, z, t) e^{-i\omega_{eg}t},$$
$$\dot{b}_e(t) = \frac{1}{i\hbar} a_g(t) \hat{\mathcal{H}}_{eg}(\xi, z, t) e^{i\omega_{eg}t}.$$

Time evolution equation of ρ_{gg} may be derived as follows

$$\begin{aligned}\frac{d\rho_{gg}}{dt} &= \frac{da_g(t)}{dt}a_g^*(t) + a_g(t)\frac{da_g^*(t)}{dt} \\ &= \frac{1}{i\hbar}b_e(t)a_g^*(t)\hat{\mathcal{H}}_{ge}(\xi,z,t)e^{-i\omega_{eg}t} + \frac{1}{-i\hbar}b_e^*(t)a_g(t)\hat{\mathcal{H}}_{eg}(\xi,z,t)e^{i\omega_{eg}t}. \end{aligned} \tag{4.4}$$

On substituting the electric field Eq.(4.3) into the interaction Hamiltonian Eq.(4.2), we obtain

$$\begin{aligned}\hat{\mathcal{H}}_{int}(\xi,z,t) &= |e|\langle g|\xi|e\rangle \cdot \boldsymbol{\mathcal{E}}(z,t) \\ &= \frac{-\hbar}{2}\Omega_{ge}^o(f(z,t)+\tilde{f}(z,t)) \\ &= \hat{\mathcal{H}}_{ge}(\xi,z,t),\end{aligned} \tag{4.5}$$

where

$$\Omega_{ge}^o = \frac{-|e|\mathcal{E}_0}{\hbar}\langle g|\xi|e\rangle,$$

is the Rabi frequency. We define the space- and time-dependent Rabi frequency as

$$\Omega_{ge}(z,t) = \Omega_{ge}^o \sum_{n=0}^{N-1} e^{-\frac{(t+\frac{z}{c}-nT_{rep})^2}{2\tau^2}+in\phi}. \tag{4.6}$$

Now substitution of Eq.(4.5) into Eq.(4.4) gives

$$\begin{aligned}\frac{d\rho_{gg}}{dt} =& \frac{i}{2}\rho_{eg}\Omega_{ge}(f(z,t)+\tilde{f}(z,t))e^{-i\omega_{eg}t} \\ &- \frac{i}{2}\rho_{ge}\Omega_{eg}(\tilde{f}(z,t)+f(z,t))e^{+i\omega_{eg}t},\end{aligned}$$

where we replaced the probability amplitudes by the appropriate notation of the elements of the density matrix. We can simplify the preceding expression further by

applying the rotating wave approximation[1]

$$\frac{d\rho_{gg}}{dt} = \frac{i}{2}\rho_{eg}\Omega_{ge}(z,t)e^{i(k_L z+\delta t)} - \frac{i}{2}\rho_{ge}\Omega_{eg}(z,t)e^{-i(k_L z+\delta t)}.$$

Here we have extracted the exponential term that contains the laser frequency and wave vector to add it to the exponential term that contains the transition frequency, then we used the expression for the detuning $\delta = \omega_L - \omega_{eg}$ to rewrite it in a compact form.

The summation in Eq.(4.6) for the Rabi frequency has the implicit comb structure in it. It states that for a two level atom interacting with a train of ultrashort pulses, the Rabi frequency is time- and space-dependent.

When we apply the same procedure to the remaining elements of the density matrix, we obtain the optical Bloch equations (OBEs) which describe the time evolution of the elements of the density matrix.

Up to this point we have not included the spontaneous decay terms. They have to be added as follows. As the excited state decays to the ground state, the excited state loss of population adds to the population of the ground state. Consequently, we have to add $+\gamma\rho_{ee}$ to the time evolution equation of ρ_{gg} and $-\gamma\rho_{ee}$ to the OBE for ρ_{ee}, where γ is the radiative decay rate [40]. The relaxation rate of the atomic coherences is represented by

$$\gamma_{coherence} = \frac{\gamma}{2} + 2\gamma_{phase},$$

where $\gamma/2$ is the contribution of the spontaneous decay of excited state, while $2\gamma_{phase}$ accounts for all other possible mechanisms of relaxation of the atom. Therefore, we

---

[1]See Appendix B for more details on the rotating wave approximation.

add $-\frac{\gamma}{2}\rho_{eg}$ and $-\frac{\gamma}{2}\rho_{ge}$ to the OBEs for ρ_{eg} and ρ_{ge}, respectively.
The OBEs are then

$$\begin{aligned}
\frac{d\rho_{gg}}{dt} &= \frac{i}{2}(\rho_{eg}\Omega_{ge}(z,t)e^{i(k_L z+\delta t)} - \rho_{ge}\Omega_{eg}(z,t)e^{-i(k_L z+\delta t)}) + \gamma\rho_{ee},\\
\frac{d\rho_{ee}}{dt} &= \frac{i}{2}(\rho_{ge}\Omega_{eg}(z,t)e^{-i(k_L z+\delta t)} - \rho_{eg}\Omega_{ge}(z,t)e^{+i(k_L z+\delta t)}) - \gamma\rho_{ee},\\
\frac{d\rho_{ge}}{dt} &= \frac{i}{2}\Omega_{ge}(z,t)e^{+i(k_L z+\delta t)}(\rho_{ee}-\rho_{gg}) - \frac{\gamma}{2}\rho_{ge},\\
\frac{d\rho_{eg}}{dt} &= \frac{i}{2}\Omega_{eg}(z,t)e^{-i(k_L z+\delta t)}(\rho_{gg}-\rho_{ee}) - \frac{\gamma}{2}\rho_{eg}.
\end{aligned}$$

As discussed at the beginning of this section, that laser cooling depends on the dissipative forces that are velocity dependent. From the quantum mechanical point of view, these forces arise as a result of the quantum mechanical momentum exchange between the atom and the laser field in the presence of spontaneous relaxation. The change in the momentum comes from the processes of photon absorption and emission. Therefore, the radiation forces is a function of the coordinates and the velocity of the center of mass of the atom [41, 42].

At this step we need to incorporate the atomic velocity into the OBEs, which can be accomplished using the hydrodynamic derivative

$$\frac{d}{dt} = \frac{\partial}{\partial t} + v\frac{\partial}{\partial z}.$$

The resulting equations of motion for the density matrix elements are

$$\frac{\partial \rho_{gg}}{\partial t} + v\frac{\partial \rho_{gg}}{\partial z} = +\gamma\rho_{ee} + \frac{i}{2}(\tilde{\rho}_{eg}\Omega_{ge}(z,t) - \tilde{\rho}_{ge}\Omega_{eg}(z,t)),$$
$$\frac{\partial \rho_{ee}}{\partial t} + v\frac{\partial \rho_{ee}}{\partial z} = -\gamma\rho_{ee} + \frac{i}{2}(\tilde{\rho}_{ge}\Omega_{eg}(z,t) - \tilde{\rho}_{eg}\Omega_{ge}(z,t)),$$
$$\frac{\partial \tilde{\rho}_{ge}}{\partial t} + v\frac{\partial \tilde{\rho}_{ge}}{\partial z} = -(\frac{\gamma}{2} + i(\delta + kv))\tilde{\rho}_{ge} + \frac{i}{2}\Omega_{ge}(z,t)(\rho_{ee} - \rho_{gg}),$$
$$\frac{\partial \tilde{\rho}_{eg}}{\partial t} + v\frac{\partial \tilde{\rho}_{eg}}{\partial z} = -(\frac{\gamma}{2} - i(\delta + kv))\tilde{\rho}_{eg} + \frac{i}{2}\Omega_{eg}(z,t)(\rho_{gg} - \rho_{ee}).$$

Here we used the substitutions

$$\tilde{\rho}_{eg} = \rho_{eg}e^{i(k_L z + \delta t)},$$
$$\tilde{\rho}_{ge} = \tilde{\rho}^*_{eg},$$

and

$$\frac{d\tilde{\rho}_{eg}}{dt} = (\frac{\partial}{\partial t} + v\frac{\partial}{\partial z})(\rho_{eg}e^{i(kz+\delta t)}),$$
$$= e^{i(kz+\delta t)}(\frac{\partial}{\partial t} + v\frac{\partial}{\partial z})\rho_{eg} + (i\delta + ikv)\rho_{eg}e^{i(kz+\delta t)}.$$

We want to simplify these partial differential equations by converting them to a system of ordinary differential equations by the method of characteristics [43]. If we consider the center of mass motion semiclassically, the trajectory is fixed $z = z_0 + vt$. We define the dependence of the density matrix elements along the trajectory as

$$\rho_{\alpha\beta}(z,t) = \varrho_{\alpha\beta}(z_0 + vt, t)\delta(z - [z_0 + vt])$$
$$= \varrho_{\alpha\beta}(t)\delta(z - [z_0 + vt]).$$

Using this substitution in the OBEs gives, for example, for the l.h.s. of ρ_{gg} equation

of motion

$$\begin{aligned}\frac{\partial \rho_{gg}}{\partial t} + v\frac{\partial \rho_{gg}}{\partial z} &= \frac{\partial(\varrho_{gg}(t)\delta(z-[z_0+vt]))}{\partial t} + v\frac{\partial(\varrho(t)_{gg}\delta(z-[z_0+vt]))}{\partial z} \\ &= \delta(z-[z_0+vt])\frac{\partial \varrho_{gg}(t)}{\partial t} - v\varrho_{gg}(t)\delta'(z-[z_0+vt]) \\ &\quad + v\varrho_{gg}(t)\delta'(z-[z_0+vt) \\ &= \delta(z-[z_0+vt])\frac{\partial \varrho_{gg}(t)}{\partial t}.\end{aligned}$$

Therefore, the time evolution equation of ϱ_{gg} is

$$\begin{aligned}\delta(z-[z_0+vt])\frac{\partial \varrho_{gg}(t)}{\partial t} = &+ \gamma\varrho_{ee}(t)\delta(z-[z_0+vt]) + \frac{i}{2}(\tilde{\varrho}_{eg}(t)\delta(z-[z_0+vt])\Omega_{ge}(z,t) \\ &- \tilde{\varrho}_{ge}(t)\delta(z-[z_0+vt])\Omega_{eg}(z,t)).\end{aligned}$$

This approach reduces the OBEs from a set of partial differential equations to a set of ordinary differential equations along the trajectory

$$\dot{\varrho}_{gg} = +\gamma\varrho_{ee} + \frac{i}{2}(\tilde{\varrho}_{eg}\Omega_{ge}(z_0+vt,t) - \tilde{\varrho}_{ge}\Omega_{eg}(z_0+vt,t)), \tag{4.7a}$$

$$\dot{\varrho}_{ee} = -\gamma\varrho_{ee} + \frac{i}{2}(\tilde{\varrho}_{ge}\Omega_{eg}(z_0+vt,t) - \tilde{\varrho}_{eg}\Omega_{ge}(z_0+vt,t)), \tag{4.7b}$$

$$\dot{\tilde{\varrho}}_{ge} = -(\frac{\gamma}{2} + i(\delta + k_L v))\tilde{\varrho}_{ge} + \frac{i}{2}\Omega_{ge}(z_0+vt,t)(\varrho_{ee} - \varrho_{gg}), \tag{4.7c}$$

$$\dot{\tilde{\varrho}}_{eg} = -(\frac{\gamma}{2} - i(\delta + k_L v))\tilde{\varrho}_{eg} + \frac{i}{2}\Omega_{eg}(z_0+vt,t)(\varrho_{gg} - \varrho_{ee}). \tag{4.7d}$$

If the initial conditions are known, the populations of the ground state and the excited state may be easily found by the direct integration of the preceding OBEs. The computer code for numerical integration is attached in Appendix D, and it utilizes the adaptive Runge-Kutta method for solving systems of coupled ordinary differential equations [44].

4.3 Radiation Force due to Laser pulse Train

The radiation force on an atom is caused by the quantum mechanical exchange of momentum between the atom and the resonant laser field. Therefore, the general quantum mechanical relation that determines the time derivative of the expectation value of the quantum mechanical variable of atomic momentum $\mathbf{P}$ is (see Ref. [42, 45])

$$\langle \mathbf{F}_z \rangle = \frac{d\langle \mathbf{P}_z \rangle}{dt} = -\frac{i}{\hbar}\langle [\mathbf{P}_z, \hat{\mathcal{H}}_{int}] \rangle,$$

where $\hat{\mathcal{H}}_{int}$ is the interaction Hamiltonian defined in Eq.(4.2). The commutator of $\mathbf{P}_z$ and $\hat{\mathcal{H}}_{int}$ is

$$[\mathbf{P}_z, \hat{\mathcal{H}}_{int}] = -i\hbar\langle \frac{\partial \hat{\mathcal{H}}_{int}}{\partial z} \rangle.$$

The force on an atom is thus given by

$$\mathbf{F}_z = -\langle \frac{\partial \hat{\mathcal{H}}_{int}}{\partial z} \rangle. \tag{4.8}$$

This relation is an example of the Ehrenfest theorem [35]. It is a quantum mechanical analogue of the classical expression, the force being the negative gradient of the potential. In the classical limit, this relation determines the classical force exerted on an atom in the radiation field, which is called the radiation force.

To find the radiation force when atoms interact with laser pulses, we consider the interaction Hamiltonian $\hat{\mathcal{H}}_{int}$ between the atoms and the laser field. This interaction operator is expressed here, as before in Chapter 3, as

$$\hat{\mathcal{H}}_{int}(\xi, z, t) = -\hat{D}(\xi) \cdot \boldsymbol{\mathcal{E}}(z, t), \tag{4.9}$$

where $D(\xi)$ is the operator of the atomic dipole moment.

The calculation of the mean value in Eq.(4.8) is reduced to evaluating the integral

$$\mathbf{F}_z = -\int_{-\infty}^{+\infty} \Psi^*(\xi,t)\frac{\partial\hat{\mathcal{H}}_{int}(\xi,z)}{\partial z}\Psi(\xi,t)d\xi, \tag{4.10}$$

On substituting Eq.(4.9) into Eq.(4.10), we obtain

$$\mathbf{F}_z = \int_{-\infty}^{+\infty} \Psi^*(\xi,t)\frac{\partial[\hat{D}(\xi)\cdot\boldsymbol{\mathcal{E}}(z,t)]}{\partial z}\Psi(\xi,t)d\xi,$$

Moreover, the wave function expansion is

$$\Psi(\xi,t) = a_g e^{-i\omega_g t}\phi_g(\xi) + b_e e^{-i\omega_e t}\phi_e(\xi),$$

Thus, the force equation after the rearrangement reads

$$\begin{aligned}
\mathbf{F}_z = &\int_{-\infty}^{+\infty} a_g^* e^{i\omega_g t}\phi_g^*(\xi)\frac{\partial[\hat{D}(\xi)\cdot\boldsymbol{\mathcal{E}}(z,t)]}{\partial z}a_g e^{-i\omega_g t}\phi_g(\xi)d\xi \\
&+\int_{-\infty}^{+\infty} a_g^* e^{i\omega_g t}\phi_g^*(\xi)\frac{\partial[\hat{D}(\xi)\cdot\boldsymbol{\mathcal{E}}(z,t)]}{\partial z}b_e e^{-i\omega_e t}\phi_e(\xi)d\xi \\
&+\int_{-\infty}^{+\infty} b_e^* e^{i\omega_e t}\phi_e^*(\xi)\frac{\partial[\hat{D}(\xi)\cdot\boldsymbol{\mathcal{E}}(z,t)]}{\partial z}a_g e^{-i\omega_g t}\phi_g(\xi)d\xi \\
&+\int_{-\infty}^{+\infty} b_e^* e^{i\omega_e t}\phi_e^*(\xi)\frac{\partial[\hat{D}(\xi)\cdot\boldsymbol{\mathcal{E}}(z,t)]}{\partial z}b_e e^{-i\omega_e t}\phi_e(\xi)d\xi.
\end{aligned}$$

The first and the forth terms on the r.h.s vanish as there is no dipole moment connecting the same electronic state. Hence, the mean force equation is

$$\begin{aligned}
\mathbf{F}_z = &\int_{-\infty}^{+\infty} a_g^* e^{i\omega_g t}\phi_g^*(\xi)\frac{\partial[\hat{D}(\xi)\cdot\boldsymbol{\mathcal{E}}(z,t)]}{\partial z}b_e e^{-i\omega_e t}\phi_e(\xi)d\xi \\
&+\int_{-\infty}^{+\infty} b_e^* e^{i\omega_e t}\phi_e^*(\xi)\frac{\partial[\hat{D}(\xi)\cdot\boldsymbol{\mathcal{E}}(z,t)]}{\partial z}a_g e^{-i\omega_g t}\phi_g(\xi)d\xi.
\end{aligned}$$

Here the electric field is for a train of ultrashort laser pulses, and it is given by

Eq.(4.3). After extracting the laser frequency and wave vector exponential terms from the electric field and applying the rotating wave approximation by neglecting the antiresonant terms (i.e. $\omega = \omega_L + \omega_e - \omega_g$) as before, the preceding force equation reads

$$\begin{aligned}\mathbf{F}_z = &\int_{-\infty}^{+\infty} a_g^* e^{i\omega_g t}\phi_g^*(\xi)\frac{\partial[\hat{D}(\xi)\cdot\boldsymbol{\mathcal{E}}_{train}(z,t)]}{\partial z}e^{i(k_L z+\omega_L t)}b_e e^{-i\omega_e t}\phi_e(\xi)d\xi \\ &+\int_{-\infty}^{+\infty} b_e^* e^{i\omega_e t}\phi_e^*(\xi)\frac{\partial[\hat{D}(\xi)\cdot\boldsymbol{\mathcal{E}}_{train}(z,t)]}{\partial z}e^{-i(k_L z+\omega_L t)}a_g e^{-i(\omega_g t}\phi_g(\xi)d\xi,\end{aligned}$$

where

$$\boldsymbol{\mathcal{E}}_{train}(z,t) = \frac{\mathcal{E}_0}{2}\sum_{n=0}^{N-1} e^{-\frac{(t+\frac{z}{c}-nT_{rep})^2}{2\tau^2}+in\phi}.$$

The Rabi frequency for a train of pulses is written in the explicit form in Eq.(4.6) as

$$\begin{aligned}\Omega_{eg}(z,t) &= \Omega_{eg}^o\sum_{n=0}^{N-1} e^{-\frac{(t+\frac{z}{c}-nT_{rep})^2}{2\tau^2}+in\phi} \\ &= \frac{2\langle e|\hat{D}(\xi)\cdot\boldsymbol{\mathcal{E}}_{train}(z,t)|g\rangle}{\hbar} \\ &= \frac{2}{\hbar}\int_{-\infty}^{+\infty}\phi_e^*(\xi)[\hat{D}(\xi)\cdot\boldsymbol{\mathcal{E}}_{train}(z,t)]\phi_g(\xi)d\xi,\end{aligned}$$

and the detuning $\delta = \omega_L - \omega_e + \omega_g$. We can use these substitutions in the preceding force equation to write it in the more compact form

$$\mathbf{F}_z = \frac{\hbar}{2}\frac{\partial}{\partial z}[(a_g^* b_e e^{i(k_L z+\delta t)})\Omega_{ge}(z,t) + (b_e^* a_g e^{-i(k_L z+\delta t)})\Omega_{eg}(z,t)].$$

With the substitution introduced in Sec.(4.3), for $\tilde{\rho}_{eg}$

$$\tilde{\rho}_{eg} = \rho_{eg}e^{i(k_L z+\delta t)} = a_g^* b_e e^{i(k_L z+\delta t)},$$

the final radiation force is

$$\mathbf{F}_z = \frac{\hbar}{2}\frac{\partial}{\partial z}[\tilde{\rho}_{eg}\Omega_{ge}(z,t) + \tilde{\rho}^*_{eg}\Omega_{eg}(z,t)]. \tag{4.11}$$

From the last equation, the force depends on the optical coherence between the ground state and the excited state. Since the Rabi frequency is not constant, the force depends also on the interaction time and position of the moving atom.

Chapter 5

Interaction of ^{23}Na Atoms with a Single Laser Pulse

5.1 Problem Set-Up

In the previous sections we developed the formalism needed to calculate the population of the energy states and the radiation force when atoms scatter light as they interact with it. Here we apply these equations to the case of a two-level atom moving in the positive z direction with velocity v_z. A typical example is the sodium transition $3S_{1/2}-3P_{3/2}$ depicted in Fig.(5.1) with the hyperfine structure characterized by the total angular momentum[1] F. The absorption takes place on the transition $3S_{1/2} \rightarrow 3P_{3/2}$ and the radiative relaxation from the excited level $3P_{3/2}$ terminates only on the initial level $3S_{1/2}$. The population is then never transferred to levels other than $3S_{1/2}$ or $3P_{3/2}$. If we choose the driving laser to be tuned to the transition $F_S = 2 \rightarrow F_P = 3$, the only allowed relaxation transition is therefore $F_P = 3 \rightarrow F_S = 2$ that fulfills the selection rule $\Delta F = 0, \pm 1$ [46, 47]. The atomic beam of Na is interacting with a

[1]The total angular momentum **F** is the vector sum of the spin angular momentum **S**, the orbital angular momentum **L**, and the nuclear spin **I**.

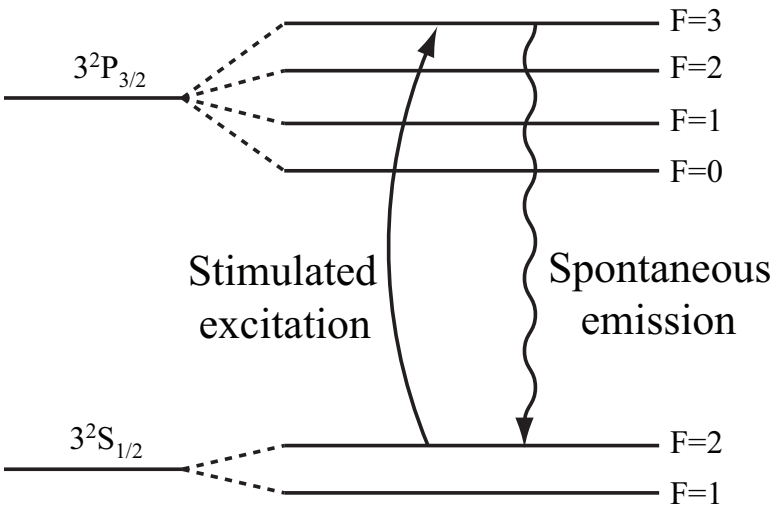

Figure 5.1: Hyperfine structure of ^{23}Na showing the transition $3S_{1/2} - P_{3/2}$. A two level system is achieved by tuning the incident laser frequency to pump the population from the hyperfine level with total angular momentum F=2 in the $3S_{1/2}$ level to the hyperfine level with total angular momentum F=3 in the $3P_{3/2}$ level.

counterpropagating train of laser pulses. Each pulse has a Gaussian envelope with FWHM $\tau_{FWHM} = 2\sqrt{2\ln 2}\tau = 230$ fs.

Now we need to find the proper value of the Rabi frequency to be used in our numerical calculations. From the pulse area theorem [48], when the area under the envelope of the Rabi frequency is $\theta = \pi/10$, each pulse will be able to transfer 1/10 of the population in the ground state to the excited state. Consequently, the required Rabi frequency may be estimated from area theorem equation

$$\theta = \frac{\pi}{10} = \int_{-\infty}^{\infty} \Omega_{eg}^{o} \mathrm{g}(t) dt,$$

where g is the pulse envelope, and the integration $\int_{-\infty}^{\infty} \mathrm{g}(t)dt = \sqrt{2\pi}\tau$ for a single Gaussian pulse. Therefore, the Rabi frequency is $\Omega_{eg}^{o} \sim 1.2 \times 10^{12}$ Hz, which in the units of the radiative decay rate of the excited state is $\Omega_{eg}^{o} \sim 10^4\gamma$.

In this chapter we discuss the interaction of the first pulse of the train with the

atoms, and in the next chapter we consider the interaction with all pulses and explore the possibility of decelerating the atomic beams using coherent pulse trains.

5.2 Coherences after the Interaction with a Single Pulse

From Eq.(4.11), the force acting on the atoms depends on the coherences; therefore, incorrect calculation of the coherences values affects the estimate of the cooling force. This is the reason beyond our interest in estimating of the coherences after interaction with the first laser pulse.

From the OBEs, Eq.(4.7c) and Eq.(4.7d), the differential equation for the coherences are

$$\dot{\tilde{\varrho}}_{eg} = -(\frac{\gamma}{2} - i(\delta + k_L v))\tilde{\varrho}_{eg} + \frac{i}{2}\Omega_{eg}(z_0 + vt, t)(\varrho_{gg} - \varrho_{ee}), \tag{5.1a}$$

$$\dot{\tilde{\varrho}}_{ge} = \dot{\tilde{\varrho}}^*_{eg}. \tag{5.1b}$$

In our calculations the Rabi frequency has the value $\Omega \sim 10^4\gamma$, which indicates that the excitation time is much shorter than the lifetime of the excited state. Therefore, we can neglect the first term in the differential equations Eq.(5.1a) as $\gamma \ll \Omega$. Additionally, all the population initially is in the ground state, then $\varrho_{gg} \approx 1$ and $\varrho_{ee} \approx 0$. Thus, the resulting differential equation for $\tilde{\varrho}_{eg}$ reduces to

$$\dot{\tilde{\varrho}}_{eg} \simeq \frac{i}{2}\Omega_{eg}(z_0 + vt, t).$$

On substituting for the Rabi frequency from Eq.(4.6) we obtain

$$\tilde{\varrho}_{eg} \simeq \frac{i}{2}\Omega^o_{eg}\int_{-\infty}^{\infty} e^{-\frac{(t+\frac{z}{c}-T_{rep})^2}{2\tau^2}}dt + C, \tag{5.2}$$

From the initial conditions $\tilde{\varrho}_{eg}(0) = 0$ and $\Omega_{eg}(0) = 0$, the integration constant $C = 0$. Although the original integration limits are $\{0, \tau_p\}$, here we can extend them to $\{-\infty, +\infty\}$ because the integrand is zero when $t < 0$ and $t > \tau$. Ultimately, the off-diagonal density matrix element $\tilde{\varrho}_{eg}$, in the weak excitation limit, and after the interaction with a single laser pulse is

$$\tilde{\varrho}_{eg} \simeq \frac{i}{2}\Omega^{o}_{eg}\sqrt{\frac{2\pi c^2\tau^2}{(c+v)^2}},$$

Now we compare the results from this analytical approach with the numerical calculation for the interaction of a single pulse with FWHM $\tau_{FWHM} = 230$ fs with an atom initially has temperature $T = 100$ K. The results are

$$\tilde{\varrho}_{eg,analytical} = 0.0779605i,$$
$$\tilde{\varrho}_{eg,numerical} = 0.07764374i.$$

These two values differ only by $\sim 0.4\%$ indicating the accuracy of our code.

5.3 Atom-Pulse Momentum Exchange

In addition to the estimate of coherences after the interaction with the first pulse, we are also interested in the momentum imparted to the atoms due to the interaction with that pulse. From Eq.(4.11), the force is

$$\begin{aligned}\mathbf{F}_z &= \frac{\hbar}{2}\frac{\partial}{\partial z}[\tilde{\rho}_{eg}\Omega^{*}_{eg}(z,t) + \tilde{\rho}^{*}_{eg}\Omega_{eg}(z,t)] \\ &= \frac{i}{2}\hbar k_L[\tilde{\rho}_{eg}\Omega^{*}_{eg}(z,t) - \tilde{\rho}^{*}_{eg}\Omega_{eg}(z,t)],\end{aligned}$$

where

$$\frac{\partial(\tilde{\rho}_{ge}\Omega_{eg}(z,t))}{\partial z} = -ik_L\tilde{\rho}_{ge}\Omega_{eg}(z,t).$$

From the Newton's second law, the total momentum transferred to the atoms is

$$\begin{aligned}\Delta p &= \int_{-\infty}^{\infty} F_z dt \\ &= \frac{i}{2}\hbar k_L \int_{-\infty}^{\infty} [\tilde{\rho}_{eg}\Omega^*_{eg}(z,t) - \tilde{\rho}^*_{eg}\Omega_{eg}(z,t)]dt.\end{aligned}$$

Using Eq.(5.2), we obtain

$$\Delta p = -\frac{1}{4}\hbar k_L|\Omega_{eg}|^2 \int_{-\infty}^{\infty} e^{-\frac{(t+\frac{z}{c}-T_{rep})^2}{2\tau^2}} \left(\int_{-\infty}^{t'} e^{-\frac{(t'+\frac{z}{c}-T_{rep})^2}{2\tau^2}} dt'\right) dt - c.c.,$$

where c.c. is the complex conjugate of the first term. Now we will express Δp in terms of the recoil momentum $\hbar k_L$. The recoil momentum $\hbar k_L$ is defined as the amount of momentum transferred to the atom due to the absorption of a single photon. Upon substituting for the appropriate values and performing the integration, the previous equation gives

$$(\frac{\Delta p}{\hbar k_L})_{analytical} = -0.00607785,$$

which is close to the value calculated from the numerical integration of the OBEs,

$$(\frac{\Delta p}{\hbar k_L})_{numerical} = -0.0060826.$$

Thus,

$$\Delta p_{error} \sim 10^{-3}\%.$$

which is a relatively negligible value. The previous calculations states that, the momentum transferred to the atoms is really small, as it corresponds to a change in the atomic velocity by the value ~ 0.15 mm/s.

In the last two sections we showed the accuracy of our approach, from the smallness of the error between the analytical and numerical calculations. This increases our confidence in the code used to integrate the OBEs; and therefore, we are ready move on to the case of the interaction of atomic beam with a train of laser pulses.

Chapter 6

Interaction of ^{23}Na Atoms with a Train of Ultrashort Laser Pulses

6.1 Problem Set-Up

In the previous chapter we showed how a single pulse is interacting with an atomic beam of sodium atoms. We found that in the weak excitation limit a single laser pulse hardly changes the atomic velocity (~ 0.15 mm/s).

In this chapter we are studying the slowing of an atomic beam of ^{23}Na atoms, by a train of ultrashort laser pulses. The laser frequency is tuned to optically pump the population from the hyperfine level $F = 2$ in the $3S_{1/2}$ energy level to the hyperfine level $F = 3$ in the $3P_{3/2}$ energy level, to achieve a two level atom, as shown in Fig.(5.1). The laser pulses of the train are identical, have Gaussian profile with a FWHM$= 2\sqrt{2\ln 2}\tau = 230$ fs, and they do not overlap. The repetition period in that train T_{rep} is 4 ns, which is smaller than the lifetime of the excited state for sodium $3P_{3/2}$ level $\tau_{rad} = 16.4$ ns.

When the first pulse interacts with the atoms, it transfers a wave packet to the excited state. After the second pulse arrives, it transfers another wave packet which

interferes with first one. As the pulses interact with the atoms, the created wave packets interfere, and build a coherent excitation.

The pulse area is set to $\theta = \pi/10$, for which we need 10 pulses to achieve the complete population inversion (CPI). The Rabi frequency is set to $\Omega^o_{eg} = 10^4\gamma$ as in the preceding chapter.

The frequency comb associated with this train of Gaussian pulses has a frequency envelope width of $1/\tau_{FWHM} = 4.3 \times 10^6$ MHz, and the separation between the comb teeth is $f_{rep} = 1/T_{rep} = 250$ MHz. Therefore, the comb envelope includes more than $17,000$ teeth. Such a broad frequency comb envelope and the large number of comb teeth will make it hard to see the difference in the adjacent comb teeth intensities. Also, we set the phase between the pulses to $\phi = 0$.

Now we are ready to solve the optical Bloch equations numerically with the enumerated parameters. The used algorithm is based on the integration by the adaptive 6^{th} order Rung-Kutta method, in which the numerical error was about 10^{-14}.

The next sections discuss the results of solving the OBEs. They present estimates to the population of the excited state due to the interaction with pulses, the radiation force on the sodium atoms, and the momentum transferred to the atomic beam.

6.2 Results

6.2.1 Population in the Excited State

In Fig.(6.1), the solid line shows the accumulation of the population in the excited state as the pulses interact with the atomic beam. It can be seen that the smallness of the repetition period ($T_{rep} < \tau_{rad}$) does not give the population enough time to completely decay to the ground state before the arrival of the second pulse. Therefore, there is an accumulation of the population in the excited state, and that is why there

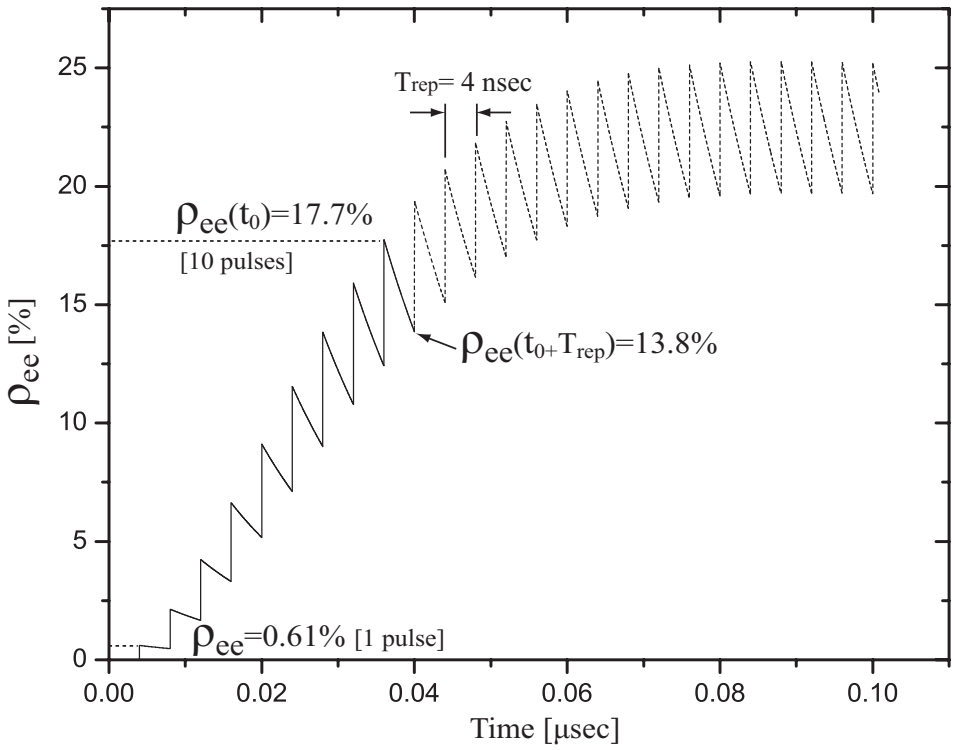

Figure 6.1: The population accumulated in the excited state due to the interaction of successive pulses with the atomic beam.

is an interference between the old and the new wave packets excited by successive laser pulses.

As seen from Fig.(6.1), the first pulse hardly perturbs the system, and excites only 0.6% of the ground state population. After the interaction with the second pulse, the total population in the excited state is almost 2.1%, which indicates that Eq.(3.11) (i.e. $|b_n(NT_{rep})|^2 = N^2|b_n(T_{rep})|^2$) holds. But after the arrival of the third pulse, the accumulated population is about 27% less than the expected from Eq.(3.11). The reason for that is, the radiative decay rate is not included in Eq.(3.11).

Also, from Fig.(6.1) we can show that in the absence of any applied signals (i.e. between the pulses), the population in the excited state level decays with time exponentially [49]

$$\rho_{ee}(t_0 + T_{rep}) = \rho_{ee}(t_0)e^{-\gamma T_{rep}}. \tag{6.1}$$

For example, we pick an arbitrary time from Fig.(6.1) as the time of maximum excitation by pulse number 10, to be our $\rho_{ee}(t_0) = 0.177$. Just before the excitation by pulse number 11, the population of the excited state decreased from 17.7% to 13.8% due to the spontaneous decay in a period equal to the repetition period of the pulses. Therefore, $\rho_{ee}(t_0 + T_{rep}) = 0.138$, and from Eq.(6.1)

$$\frac{\rho_{ee}(t_0 + T_{rep})}{\rho_{ee}(t_0)} = 0.78,$$

and $e^{-\gamma T_{rep}} = 0.78$. All these estimates and matches between results increase our confidence in the used numerical code.

6.2.2 Atom-Train Momentum Exchange

In Chapter 5 we found that a single weak pulse transfers a small amount of momentum to the atomic beam ($\sim 0.006\hbar k_L$) that hardly changes the atomic velocity (~ 0.15 mm/s). In this section we discuss the momentum exchange between the sodium atoms and a pulse train.

Consider an ideal case when sodium atoms moves in the positive z direction with velocity v_z, and they are irradiated by a coherent train of ultrashort femto-second laser pulses. The detuning of the laser frequency is set to $-k_L v_z$. In the rest frame of the atoms, the laser source is moving towards the atoms, therefore, they see the frequency of the laser is blue shifted (Doppler shifted) by the value $k_L v_z$, which compensates for the red detuning $-k_L v_z$ indicated above. Thus, the laser frequency matches the transition frequency perfectly, and a resonant interaction is achieved.

For cooling atoms we calculated the light pressure force on the atoms using Eq.(4.11), then we integrated the force over time to compute the imparted momentum

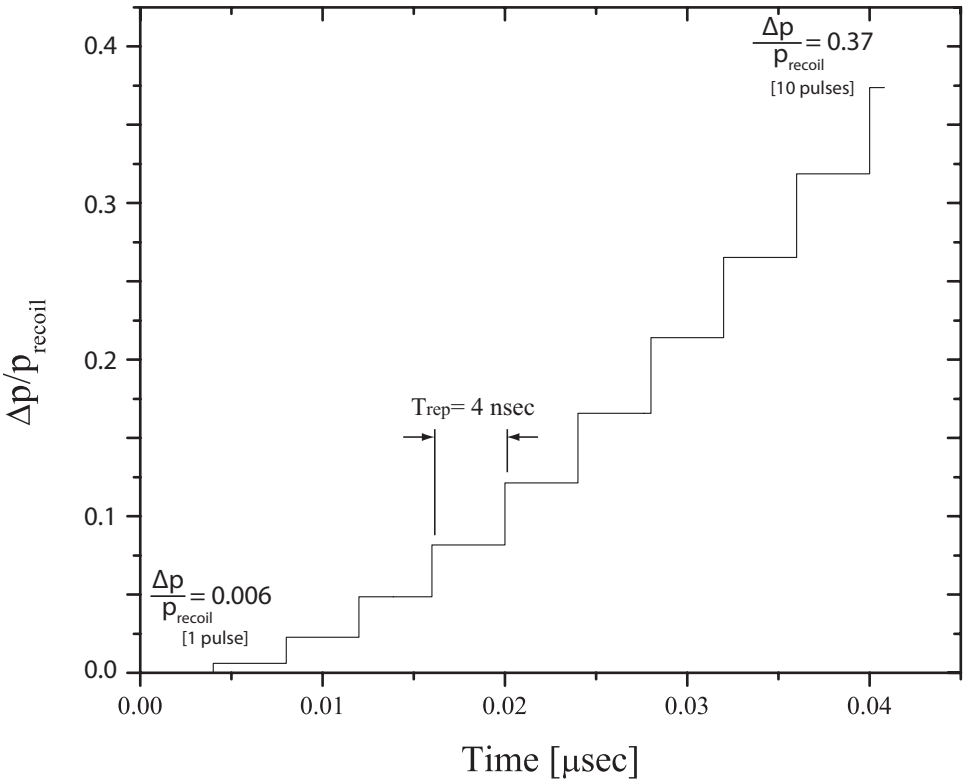

Figure 6.2: The momentum transferred to the atomic beam due to the accumulation of the population in the excited state by the individual pulses.

using

$$\Delta p = \int \mathbf{F}_z dt. \tag{6.2}$$

The results are shown in Fig.(6.2), Fig.(6.3), and Fig.(6.4).

Fig.(6.2) shows the total momentum imparted to the atoms by the train. The first pulse imparts a total momentum of $\sim 0.6\%$ of $\mathrm{p_{recoil}}$. For the case of sodium atoms, the recoil momentum (defined in Sec.(4.1)) is $\mathrm{p}_{recoil} = 1.125 \times 10^{-30}$ N $\cdot$ s, which limits the change in the velocity due to a single photon absorbtion to $v =$ 3 cm/s. Thus, the first pulse has changed the atomic velocity by an amount of ~ 0.15 mm/s which is a negligible amount due to the weakness of the pulse (see Chapter 5).

After the arrival of the second pulse, the total momentum transferred to the atoms is ~ 0.0225 $\mathrm{p_{recoil}}$, which may be predicted from Eq.(3.11) as follows.

The population transferred to the excited state by a pulse train is directly proportional to the population excited by the first pulse, and the square of the number of pulses as in Eq.(3.11)

$$|b_e(NT_{rep})|^2 = N^2|b_e(T_{rep})|^2.$$

Moreover, the force from absorbtion followed by spontaneous emission can be written as (see Ref.[45])

$$\begin{aligned} F_{sp} &= \hbar k_L \gamma \varrho_{ee}, \\ \frac{\Delta p}{\Delta t} &= \hbar k_L \frac{\Delta N}{\Delta t}. \end{aligned}$$

The previous equation is interpreted as follows. During the time interval Δt, the atoms absorbs ΔN photons and obtains a total momentum of $\Delta p = \hbar k_L \Delta N$. From quantum mechanics, the population of the excited state is directly proportional to the number absorbed photons $\Delta N \propto |b_e(t)|^2$. Therefore, we can formulate an equation for the total imparted momentum similar to Eq.(3.11) as

$$\begin{aligned} \Delta p(NT_{rep}) &\propto \hbar k_L |b_e(NT_{rep})|^2, \\ \Delta p(NT_{rep}) &= N^2 \Delta p(T_{rep}), \end{aligned} \tag{6.3}$$

where $\Delta p(T_{rep}) \propto \hbar k_L |b_e(T_{rep})|^2$ is the momentum transferred by the first pulse.

From the preceding equation, after the interaction with the third pulse we expect to have a total momentum transferred to the atom equals ~ 0.055 $\mathrm{p_{recoil}}$, which excess the actual value by 15%. Hence, Eq.(6.3) valid only for the first few pulses (i.e. for small N). It is indicated in Fig.(6.2) that, the total imparted momentum to the atoms due to the interaction of ten pulses is 0.37 $\mathrm{p_{recoil}}$, corresponding to a change in the

velocity equals ~ 1.13 cm/s.

6.2.3 Doppler Cooling Using Frequency Combs

In the previous section we showed that by using a train of ten pulses we have been able to decelerate the sodium atoms by a maximum amount of ~ 1.13 cm/s at the resonance. In this section we seek the ability to cool the atoms using pulses based on the previous discussions and results.

As stated in the beginning of the previous section, a beam of sodium atoms is interacting with a counterpropagating laser beam tuned to resonance is a typical example of Doppler cooling. The natural line width of the $3p_{3/2}$ energy level for sodium is 10 MHz, and having an effective cooling for an atomic beam of ^{23}Na atoms requires that the detuning is larger than the line width.

Fig.(6.3) shows the momentum imparted to the atoms with different Doppler shifts. It can be noticed that the maximum momentum transferred is 0.37 $\mathrm{p_{recoil}}$, as indicated before in Fig(6.2), but in this case it transfers only to a narrow group of atoms with a specific velocity. The total momentum is plotted versus the Doppler shift normalized to the frequency comb teeth separation $f_{rep} = 250$ MHz. The resulting profile, qualitatively, is similar to the comb structure discussed in Chapter 2. The atoms see different laser sources with different detunings. In the the frequency range $-1.5f_{rep} + 1.5f_{rep}$, which is plotted in Fig.(6.3), we have three comb teeth; one is located at the carrier frequency f_L, corresponding to the zero detuning, and the other two are at frequencies $f_L \pm f_{rep}$, corresponding to detunings $\delta = \pm 250$MHz, respectively. From Fig.(6.3) we observe that whenever the Doppler shift equals the detuning, the momentum transfer is maximum. When the detuning $\delta = -\gamma$, two groups of velocities are decelerating, one group has $v_z = -\delta/k_L$ (the middle teeth), and the other group has $v_z = f_{rep}/k_L - \delta/k_L$ (the right teeth). As the atoms continu-

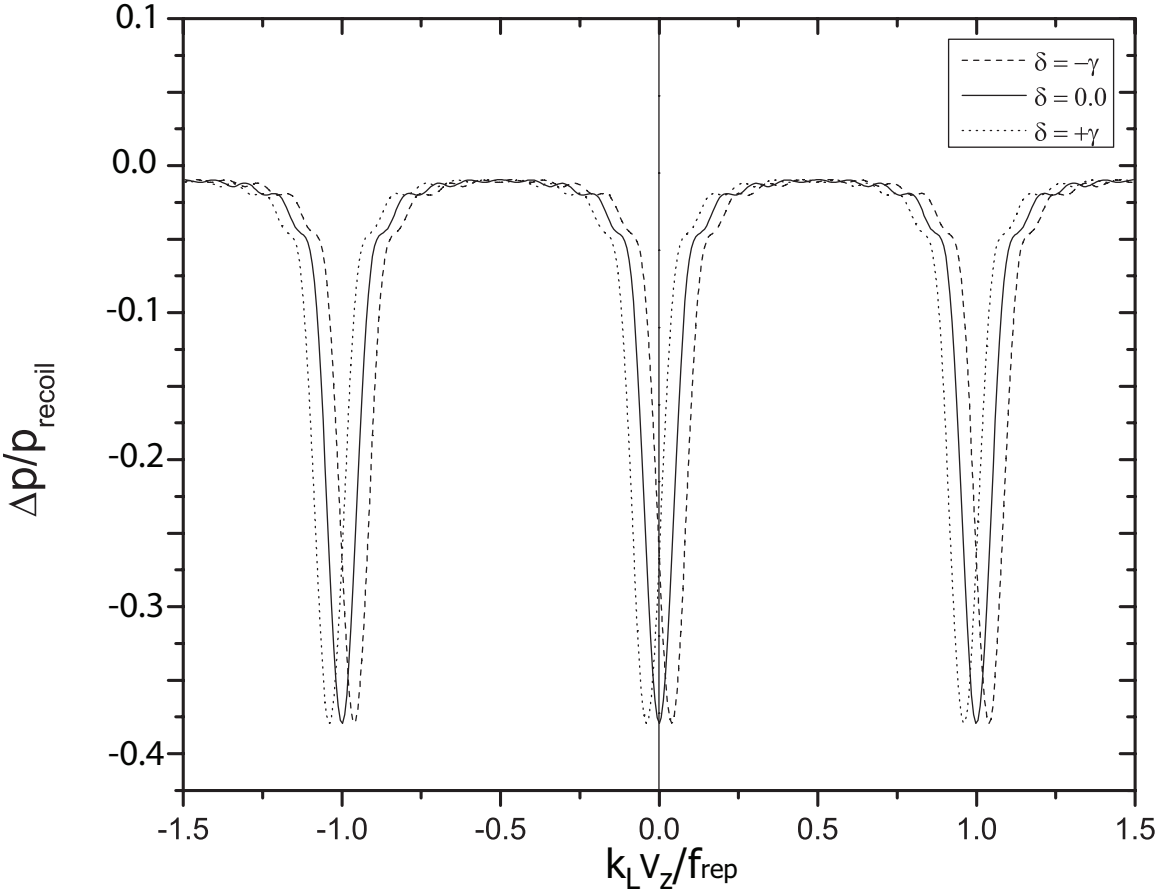

Figure 6.3: The momentum imparted to the moving atoms due to the interaction with a train of ultra short pulses. Some of the atoms are decelerated fast when their Doppler shift equals the frequency of a certain tooth "Resonance", while others are decelerated very slowly due to the "Off-Resonance" interaction.

ously slow down due to photon absorption, the Doppler shift changes and the atoms are out of resonance with the applied laser pulses. When the atoms are far enough off resonance, the rate of absorption is significantly reduced. The result is that only atoms with a proper velocity are slowed down, and they are only slowed by a small amount.

Nevertheless, this process of slowing down atoms results in a cooling or narrowing of the velocity distribution. In an atomic beam, there is typically a spread of velocities around v_{rms}. Atoms with the proper velocity will absorb rapidly and decelerate. Those with velocity $v_z > v_{rms}$ will absorb slowly, then rapidly as they come into resonance, and finally slowly as they continue to decelerate. Atoms with velocity $v_z < v_{rms}$ absorb little and decelerate little. Thus atoms from a range of velocities around the resonant velocity are pushed into a narrower range centered on a lower velocity.

Fig.(6.4) shows the main tooth interaction with the atomic beam as it approaches the zero. When atoms velocity is close to zero (i.e. $k_L v_z / f_{rep} \to 0$), the equation of the momentum imparted to the atoms behaves as (the dashed line)

$$\Delta p_{total} = \Delta p_{0(v_z=0)} - \alpha v_z, \tag{6.4}$$

which matches the equation of the force in the case of the interaction of atomic beams with the CW lasers (see Eq.(3.20) in Ref. [45])

$$F = F_0 - \beta v_z + \cdots, \tag{6.5}$$

where

$$\beta = -\hbar k^2 \frac{4 s_0 (\delta\gamma)}{(1 + s_0 + (2\delta/\gamma)^2)^2}, \tag{6.6}$$

in which $s_0 = 2|\Omega|^2/\gamma^2$, is the saturation parameter. The first term in Eq.(6.4) is

the intercept with the $\Delta p/p_{recoil}$ axis at $v_z = 0$ in Fig.(6.4), therefore, it is velocity independent. This term is the momentum transferred to the atoms at rest. It is responsible for decelerating the atomic beam then deflecting the atoms direction of motion when the atomic velocity $v_z = 0$. This term, Δp_0, corresponds to the first term F_0 in Eq.(6.5), the force on a two level atom at rest. The second term in Eq(6.4), is the momentum transferred to the atoms at motion, thus, it is velocity dependent. This term is also responsible for slowing the atoms, and ultimately, cooling them. The second term in Eq.(6.4) contains the slope α, which is analogous to the damping coefficient β introduced in Eq.(6.5) and defined in Eq.(6.6). It is obvious form Fig.(6.4) that, when the laser frequency is red detuned (i.e. $\delta < 0$, the dashed line) the coefficient α is negative, and if the laser frequency is blue detuned (i.e. $\delta > 0$, the dotted line) the coefficient α is positive. These results perfectly agree with the definition of the damping coefficient β in Eq.(6.6).

The distinction between cooling and slowing the atomic beams is as follows. Even though the momentum transferred to the atomic beam reduces the average velocity to zero, the mean squared velocity may be not zero. An atom with zero velocity is equally likely to absorb a photon from the traveling laser pulses. When this occurs, the mean squared velocity will increase. Thus, we need to decrease the mean squared velocity in addition to having an average velocity equal to zero to get an efficient cooling.

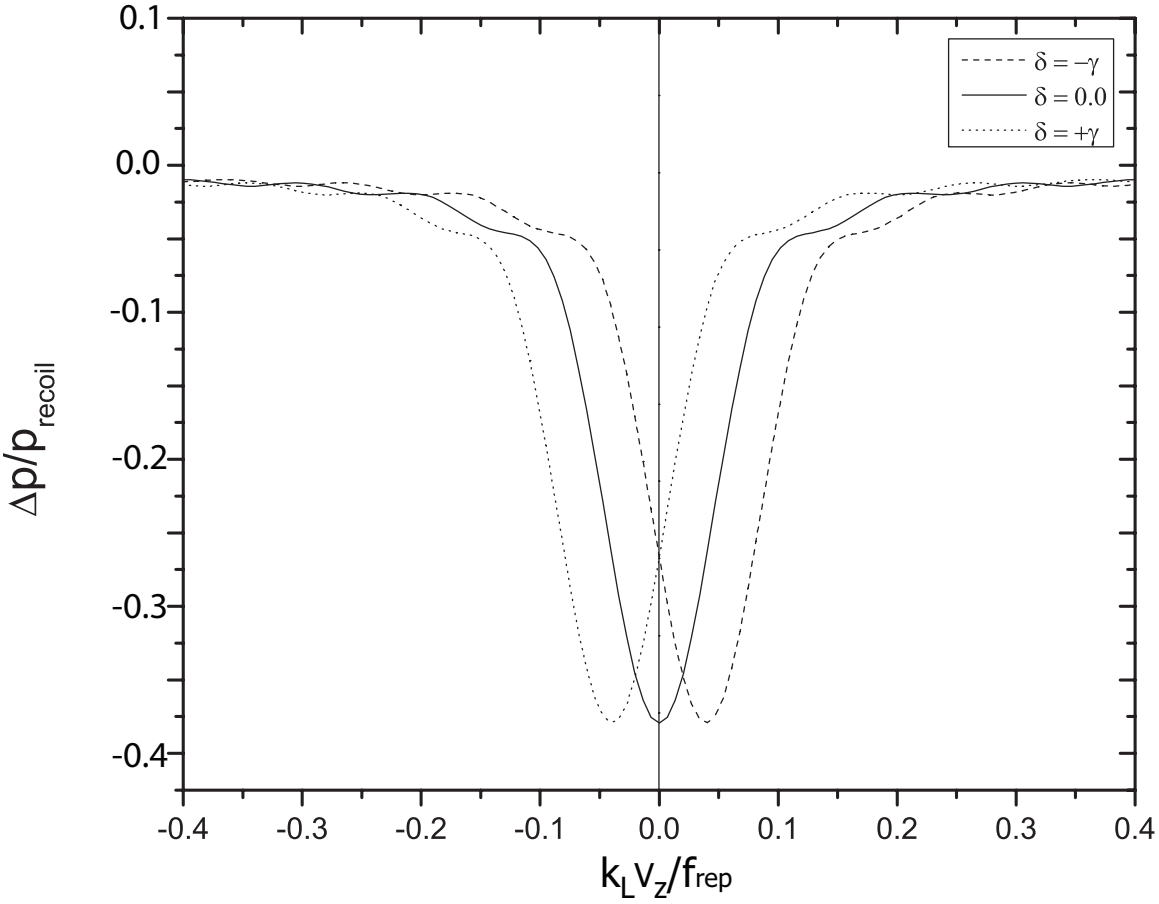

Figure 6.4: Interaction of the main comb tooth with atomic beam when its velocity is brought close to zero. The figure shows the momentum transfer to slowly moving atoms when the carrier frequency is red detuned (dashed line) and blue detuned (dotted line).

Chapter 7

Conclusion

This thesis explores the possibility of cooling atomic beams using a coherent train of ultrashort laser pulses (frequency combs). It is a preliminary step towards cooling multilevel atoms and molecules using frequency combs as they may eliminate the need for multiple laser sources required to cool mutilevel atoms.

We discussed the possibility of changing the separation between the comb teeth by changing the repetition period of the pulses in the time domain, as they are related by $T_{rep} = 1/f_{rep}$. We also mentioned in Chapter 2 the ability to move the teeth inside the comb envelope around the carrier frequency by changing the phase between the pulses. Therefore, we are able to tune the frequency comb teeth to a target transition using the repetition period and the phase between the pulses in the time domain.

In Chapter 5 we made estimates for a two-level atom interacting with a single laser pulse. We have shown that the numerical estimates of the excited state population and the momentum transferred to the atom agree with the analytical approach, for weak pulses, with a negligible percent error. We also found that when an atom interacts with a weak single laser pulse, the pulse only perturbs the population in the ground state, and transfers a small percentage of the population to the excited state. In addition to this, there is almost no change in the velocity of the atoms after the interaction.

However, as shown in Chapter 6 for an atomic beam interacting with a train of ultra-short Gaussian pulses, there is an appreciable amount of the initial population transferred to the excited state due to the coherent interference between the pulses in the train. Furthermore, although the pulses are assumed to be weak, they impart to the atoms an amount of momentum equal to 0.37 $\hbar k_L$. This transferred momentum has changed the atomic velocity by a considerable amount.

Bibliography

[1] A. Kastberg, W. D. Phillips, S. L. Rolston, R. J. C. Spreeuw, and P. S. Jessen. Adiabatic cooling of cesium to 700 nk in an optical lattice. *Phys. Rev. Lett.*, 74(9):1542–1545, Feb 1995.

[2] J. Lawall, S. Kulin, B. Saubamea, N. Bigelow, M. Leduc, and C. Cohen-Tannoudji. Three-dimensional laser cooling of helium beyond the single-photon recoil limit. *Phys. Rev. Lett.*, 75(23):4194–4197, Dec 1995.

[3] Jan Grünert and Andreas Hemmerich. Sub-doppler magneto-optical trap for calcium. *Phys. Rev. A*, 65(4):041401, Mar 2002.

[4] Grunert and A. Hemmerich. Optimizing the production of metastable calcium atoms in a magneto-optical trap. *Applied Physics B: Lasers and Optics*, 73(8):815–818, December 2001.

[5] Claudio L. Cesar, Dale G. Fried, Thomas C. Killian, Adam D. Polcyn, Jon C. Sandberg, Ite A. Yu, Thomas J. Greytak, Daniel Kleppner, and John M. Doyle. Two-photon spectroscopy of trapped atomic hydrogen. *Phys. Rev. Lett.*, 77(2):255–258, Jul 1996.

[6] F. Riehle Th. Kisters, K. Zeiske and J. Helmcke. High-resolution spectroscopy with laser-cooled and trapped calcium atoms. *Applied Physics B: Lasers and Optics*, pages 89–98, May 1994.

[7] E. Simon, P. Laurent, and A. Clairon. Measurement of the stark shift of the cs hyperfine splitting in an atomic fountain. *Phys. Rev. A*, 57(1):436–439, Jan 1998.

[8] Franco Dalfovo, Stefano Giorgini, Lev P. Pitaevskii, and Sandro Stringari. Theory of bose-einstein condensation in trapped gases. *Rev. Mod. Phys.*, 71(3):463–512, Apr 1999.

[9] H. C. Busch, M. K. Shaffer, E. M. Ahmed, and C. I. Sukenik. Trap loss in a dual-species Rb-Ar* magneto-optical trap. *Phys. Rev. A*, 73(2):023406, Feb 2006.

[10] K. B. Davis, M. O. Mewes, M. R. Andrews, N. J. van Druten, D. S. Durfee, D. M. Kurn, and W. Ketterle. Bose-einstein condensation in a gas of sodium atoms. *Phys. Rev. Lett.*, 75(22):3969–3973, Nov 1995.

[11] M. H. Anderson, J. R. Ensher, M. R. Matthews, C. E. Wieman, and E. A. Cornell. Observation of Bose-Einstein Condensation in a Dilute Atomic Vapor. *Science*, 269(5221):198–201, 1995.

[12] Z-T. Lu, C. Bowers, S. J. Freedman, B. K. Fujikawa, J. L. Mortara, S-Q. Shang, K. P. Coulter, and L. Young. Laser trapping of short-lived radioactive isotopes. *Phys. Rev. Lett.*, 72(24):3791–3794, Jun 1994.

[13] C. Y. Chen, Y. M. Li, K. Bailey, T. P. O'Connor, L. Young, and Z.-T. Lu. Ultrasensitive Isotope Trace Analyses with a Magneto-Optical Trap. *Science*, 286(5442):1139–1141, 1999.

[14] V. S. Letokhov Pis'ma Zh. Eksp. *Teor. Fiz.*, 7:348, 1968.

[15] A. P. Kazantsev Zh. Eksp. *Teor. Fiz.*, 66:1599, 1974.

[16] T.W. Hansch and A.L. Schawlow. Cooling of gases by laser radiation. *Optics Communications*, 13(1):68 – 69, 1975.

[17] D. J. Wineland, R. E. Drullinger, and F. L. Walls. Radiation-pressure cooling of bound resonant absorbers. *Phys. Rev. Lett.*, 40(25):1639–1642, Jun 1978.

[18] William D. Phillips and Harold Metcalf. Laser deceleration of an atomic beam. *Phys. Rev. Lett.*, 48(9):596–599, Mar 1982.

[19] Steven Chu, L. Hollberg, J. E. Bjorkholm, Alex Cable, and A. Ashkin. Three-dimensional viscous confinement and cooling of atoms by resonance radiation pressure. *Phys. Rev. Lett.*, 55(1):48–51, Jul 1985.

[20] E. L. Raab, M. Prentiss, Alex Cable, Steven Chu, and D. E. Pritchard. Trapping of neutral sodium atoms with radiation pressure. *Phys. Rev. Lett.*, 59(23):2631–2634, Dec 1987.

[21] Yvan Castin, Kirstine Berg-So/rensen, Jean Dalibard, and Klaus Mo/lmer. Two-dimensional sisyphus cooling. *Phys. Rev. A*, 50(6):5092–5115, Dec 1994.

[22] G. Anetsberger O. Arcizet A. Schliesser, R. Rivire and T. J. Kippenberg. Resolved-sideband cooling of a micromechanical oscillator. *Nature Physics*, 4:415 – 419, Apr 2008.

[23] Peter Horak, Gerald Hechenblaikner, Klaus M. Gheri, Herwig Stecher, and Helmut Ritsch. Cavity-induced atom cooling in the strong coupling regime. *Phys. Rev. Lett.*, 79(25):4974–4977, Dec 1997.

[24] Mark Kasevich and Steven Chu. Laser cooling below a photon recoil with three-level atoms. *Phys. Rev. Lett.*, 69(12):1741–1744, Sep 1992.

[25] Kathryn Moler, David S. Weiss, Mark Kasevich, and Steven Chu. Theoretical analysis of velocity-selective raman transitions. *Phys. Rev. A*, 45(1):342–348, Jan 1992.

[26] J. Reichel, F. Bardou, M. Ben Dahan, E. Peik, S. Rand, C. Salomon, and C. Cohen-Tannoudji. Raman cooling of cesium below 3 nk: New approach inspired by lévy flight statistics. *Phys. Rev. Lett.*, 75(25):4575–4578, Dec 1995.

[27] Blinov et al. Broadband laser cooling of trapped atoms with ultrafast pulses. *Opt. Soc. Am. B*, 23(6), June 2006.

[28] Carmen M. Tesch and Regina de Vivie-Riedle. *Phys. Rev. Lett.*, 89:157901, 2002.

[29] Carmen M. Tesch and Regina de Vivie-Riedle. *quant-ph*, 1005.4144, 2010.

[30] Carmen M. Tesch and Regina de Vivie-Riedle. *J. Phys. Chem. A*, 102, 1998.

[31] R. N. Zare. *Science*, 279:1875, 1998.

[32] Gordon W.F. Drake, editor. *Springer Handbook of Atomic, Molecular, and Optical Physics*. Springer, 2005.

[33] Lus E. E. de Araujo. *Phys. Rev. A*, 77:033419, 2008.

[34] J. D. Jackson, editor. *Classical Electrodynamics Third Edition*. Wiley, 1998.

[35] Claude Cohen-Tannoudji, Bernard Diu, and Frank Laloe. *Quantum Mechanics*, volume I and II. Wiley, John & Sons, 1998.

[36] Luís E. E. de Araujo. Selective and efficient excitation of diatomic molecules by an ultrashort pulse train. *Phys. Rev. A*, 77(3):033419, Mar 2008.

[37] K. A. Suominen and B. M. Garraway. Wave-packet dynamics: Level-crossing-induced changes in momentum distributions. *Phys. Rev. A*, 48(5):3811–3819, Nov 1993.

[38] Luís E. E. de Araujo. Selective and efficient excitation of diatomic molecules by an ultrashort pulse train. *Phys. Rev. A*, 77(3):033419, Mar 2008.

[39] L. D. Landau and L. M. Lifshitz, editors. *Quantum Mechanics Non-Relativistic Theory*. Butterworth-Heinemann, 1981.

[40] Peter Lambropoulos and David Petrosyan. *Fundamentals of Quantum Optics and Quantum Information*. Springer, 2009.

[41] Vladilen Letokhov, editor. *Laser Control of Atoms and Molecules*. Oxford University Press, USA, 2007.

[42] V.G. Minogin and V.S. Letokhov, editors. *Laser Light Pressure on atoms*. Routledge,New York, 1987.

[43] Stanley J. Farlow. *Partial Differential Equations for Scientists and Engineers*. Dover Publications, 1993.

[44] Richard Hamming. *Numerical Methods for Scientists and Engineers*. Dover Publications, 1987.

[45] Harold J. Metcalf and Peter van der Straten. *Laser Cooling and Trapping*. Springer,New York, 1999.

[46] David Bohm. *Quantum theory*. Dover Publications, 1989.

[47] Wolfgang Demtröder. *An Introduction to Atomic and Molecular Physics*. Springer, 2006.

[48] Pierre Meystre and Murray Sargent. *Elements of Quantum Optics*. Springer, 1998.

[49] A. E. Siegman, editor. *Lasers*. University Science Books, 1986.

[50] Hans J. Weber George B. Arfken and Frank Harris, editors. *Mathematical Methods for Physicists*. Academic Press, 2000.

[51] Ronald Bracewell. *The Fourier Transform & Its Applications*. McGraw-Hill, 1999.

[52] L. Allen and J. H. Eberly. *Optical Resonance and Two-Level Atoms*. Dover Publications, 1987.

Appendix A

Fourier Transform of a Train of Gaussian Pulses

Consider a train of identical pulses emitted from an ideal mode-locked laser at equal time intervals and moving in the negative z direction. The repetition period of the pulses in the train is T_{rep}, defined as the separation between two successive envelopes. The electric field of the total pulse train for a general envelope g(t) is

$$\boldsymbol{\mathcal{E}}(z,t) = \frac{1}{2}\mathcal{E}_0(\sum_{n=0}^{N-1} \mathrm{g}(t - nT_{rep})e^{in\phi}e^{-i(k_L z+\omega_L t)} + c.c.).$$

The term g($t - nT_{rep}$) is the pulses envelope which are assumed to be identical, this requires that the pulse separation is an integer number of optical cycles $T_{rep} = NT_L$, ϕ is the phase shift between the consecutive pulses $\phi = \omega_L T_{rep}$.

When the envelope is in the form of a Gaussian shape

$$\mathrm{g}(t - nT_{rep}) = e^{-\frac{(t-nT_{rep})^2}{2\tau^2}},$$

the electric field train in the long-wavelength approximation[1] takes the form

$$\mathcal{E}(t) \approx \frac{1}{2}\mathcal{E}_0[\sum_{n=0}^{N-1} e^{-i\omega_L t - \frac{(t-nT_{rep})^2}{2\tau^2} + in\phi} + c.c.]. \tag{A.1}$$

We want to Fourier transform the preceding electric field equation to obtain the frequencies of the electromagnetic waves that make up $\mathcal{E}(t)$. By using the Fourier transform, which is generally calculated by [50]

$$\mathcal{E}(\omega) = \mathcal{F}[\mathcal{E}](t) = \frac{1}{\sqrt{2\pi}} \int_{-\infty}^{\infty} \mathcal{E}(t) e^{i\omega t} dt,$$

the Fourier transform of the first pulse in the train, corresponding to $n = 0$ in both summations on the r.h.s. of Eq.(A.1), are

$$\begin{aligned} F_1^+(\omega) =& \frac{1}{2}\tau\mathcal{E}_0 e^{-\frac{1}{2}\tau^2(\omega-\omega_L)^2}, \\ F_1^-(\omega) =& \frac{1}{2}\tau\mathcal{E}_0 e^{-\frac{1}{2}\tau^2(\omega+\omega_L)^2}, \end{aligned}$$

With the use of the shift theorem [51], we can find the Fourier transform for all pulses in the train. Therefore, the electric field in the frequency-domain for a train consisted of N pulses is

$$\mathcal{E}(\omega) = [F_1^+(\omega) \sum_{n=0}^{N-1} e^{in(\phi + T_{rep}(\omega-\omega_L))} + F_1^-(\omega) \sum_{n=0}^{N-1} e^{-in(\phi - T_{rep}(\omega+\omega_L))}].$$

This is the equation for the electric field in the frequency domain. Simplifying both

---

[1]For atomic systems, the relevant length scale for the particles is approximately determined by the atomic Bohr radius ($a_0 = 0.5$ $\mathring{A}$), which is typically four orders of magnitude smaller than the optical wavelengths that determine the characteristic length scale of the optical fields. Therefore, in the long-wavelength approximation $\mathbf{k} \cdot \mathbf{r} \to 0$, and $e^{-i\mathbf{k}\cdot\mathbf{r}} \approx 1$.

summations further by treating each of them as the first N terms in geometrical series

$$\sum_{n=0}^{N-1} e^{in(\frac{\phi}{T_{rep}}+(\omega-\omega_L))T_{rep}} = 1 + e^{i(\frac{\phi}{T_{rep}}+(\omega-\omega_L))T_{rep}} + \cdots + e^{i(N-1)(\frac{\phi}{T_{rep}}+(\omega-\omega_L))T_{rep}}. \quad \text{(A.2)}$$

On multiplying both sides of Eq.(A.2) by

$$e^{i(\frac{\phi}{T_{rep}}+(\omega-\omega_L))T_{rep}},$$

we obtain

$$e^{i(\frac{\phi}{T_{rep}}+(\omega-\omega_L))T_{rep}} \cdot S_n(\omega) = e^{i(\frac{\phi}{T_{rep}}+(\omega-\omega_L))T_{rep}}[1 + e^{i(\frac{\phi}{T_{rep}}+(\omega-\omega_L))T_{rep}} + \cdots + e^{i(N-1)(\frac{\phi}{T_{rep}}+(\omega-\omega_L))T_{rep}}], \quad \text{(A.3)}$$

where

$$S_n(\omega) = \sum_{n=0}^{N-1} e^{in(\frac{\phi}{T_{rep}}+(\omega-\omega_L))T_{rep}}.$$

Subtracting Eq.(A.3) from Eq.(A.2) to obtain

$$(1 - e^{i(\frac{\phi}{T_{rep}}+(\omega-\omega_L))T_{rep}})S_n(\omega) = 1 - e^{iN(\frac{\phi}{T_{rep}}+(\omega-\omega_L))T_{rep}},$$

therefore, the summation $S_n(\omega)$ has the compact form

$$S_n(\omega) = \frac{1 - e^{iN(\frac{\phi}{T_{rep}}+(\omega-\omega_L))T_{rep}}}{1 - e^{i(\frac{\phi}{T_{rep}}+(\omega-\omega_L))T_{rep}}}.$$

The last equation is simplified further on multiplying the numerator and the denominator by

$$e^{-\frac{i}{2}(\frac{\phi}{T_{rep}}+(\omega-\omega_L))T_{rep}} \cdot e^{-i\frac{N}{2}(\frac{\phi}{T_{rep}}+(\omega-\omega_L))T_{rep}},$$

which results in

$$S_n(\omega) = \frac{e^{-\frac{i}{2}(\frac{\phi}{T_{rep}}+(\omega-\omega_L))T_{rep}}\big[e^{i\frac{N}{2}(\frac{\phi}{T_{rep}}+(\omega-\omega_L))T_{rep}} - e^{-i\frac{N}{2}(\frac{\phi}{T_{rep}}+(\omega-\omega_L))T_{rep}}\big]}{e^{-i\frac{N}{2}(\frac{\phi}{T_{rep}}+(\omega-\omega_L))T_{rep}}\big[e^{\frac{i}{2}(\frac{\phi}{T_{rep}}+(\omega-\omega_L))T_{rep}} - e^{-\frac{i}{2}\frac{\phi}{T_{rep}}+(\omega-\omega_L))T_{rep}}\big]}.$$

Making the substitution $\zeta = \frac{\phi}{T_{rep}} + (\omega - \omega_L)$ for further simplification

$$S_n(\omega) = e^{\frac{i}{2}(N-1)\zeta T_{rep}}\frac{\big[e^{i\frac{N}{2}\zeta T_{rep}} - e^{-i\frac{N}{2}\zeta T_{rep}}\big]}{\big[e^{\frac{i}{2}\zeta T_{rep}} - e^{-\frac{i}{2}\zeta T_{rep}}\big]}.$$

Using the substitution for the sin function

$$\sin(\zeta T_{rep}) = \frac{1}{2i}(e^{i\zeta T_{rep}} - e^{-i\zeta T_{rep}}),$$

thus, the summation has the simple form

$$\sum_{n=0}^{N-1} e^{in\zeta T_{rep}} = \frac{\sin(\frac{N}{2}\zeta T_{rep})}{\sin(\frac{\zeta T_{rep}}{2})}. \tag{A.4}$$

Similarly, the second summation has the form

$$\sum_{n=0}^{N-1} e^{in\eta T_{rep}} = \frac{\sin(\frac{N}{2}\eta T_{rep})}{\sin(\frac{\eta T_{rep}}{2})},$$

where

$$\eta = (\omega + \omega_L) - \frac{\phi}{T_{rep}}.$$

Ultimately, the final electric field profile in the frequency-domain is

$$\mathcal{E}(\omega) = [F_1^+(\omega)\frac{\sin(\frac{N}{2}\zeta T_{rep})}{\sin(\frac{\zeta T_{rep}}{2})} + F_1^-(\omega)\frac{\sin(\frac{N}{2}\eta T_{rep})}{\sin(\frac{\eta T_{rep}}{2})}]. \tag{A.5}$$

Appendix B

The Rotating Wave Approximation

The time evolution equations for a two-level atom interacting with weak electromagnetic field, whether expressed in terms of amplitudes or density matrix elements, have no known exact analytical solution. An approximate solution for the interaction can be obtained using the rotating wave approximation (RWA), which was first employed by Rabi in his derivation of the "flopping formula" [48].

Under the influence of a monochromatic electromagnetic field of frequency ω_L, atoms undergo transitions between their lower and upper states by interacting with either the positive or the negative frequency part of the field. The corresponding contributions to the atomic evolution equations oscillate at frequencies $\omega_L - \omega_{eg}$ and $\omega_L + \omega_{eg}$. For near-resonant atom-field interactions, the rapidly oscillating contributions $\omega_L + \omega_{eg}$ lead to small corrections, and do not make significant contributions to the differential equations for long times. Thus, they average out.

The physical idea behind the RWA is that a linear oscillation can be decomposed into a sum of two counterrotating motions, one of which will be resonant with the precessing dipole moment (representative of the quantum mechanical transitions between two states), and the other is antiresonant, i.e., rotating opposite to that dipole precession [52].

Appendix C

Cooling Parameters of Sodium ^{23}Na

Time domain parameters:

Parameter	Value
Pulse duration	τ= 100fs = 0.1 ps
Repetition period	T_{rep}= 4 ns
Life time	τ_{rad}= 16.4 ns

Frequency domain parameters:

Parameter	Value
Radiative decay	γ_{rad}=60 MHz
Teeth spacing	Δf_{teeth}=250 MHz
Rabi Frequency at I_{peak}	$\Omega \approx 1$ THz $\approx 10^4 \gamma_{rad}$
Laser Frequency at $\delta = 0$	$\omega_L \approx 3200$ THz
Wave number	$k_L \approx 10^7 m^{-1}$

Atomic velocities for different Temperatures:

Atomic temperature(K)	Velocity of the atoms(m per s)	Doppler shift (MHz)
0	0	0
10^{-6}	0.012	0.13
10^{-3}	0.6	6.4
1	19	202.7
100	190	2026.8

Appendix D

Computer Code for Numerical Integration of the OBEs

```
PROGRAM                Laser-Cooling-Prop-ampl
!========= Constants, Variables, and Data =========
INTEGER*8 va,vb,n,j,e,g,Nr,tstep,tdel,termn,termn_Rho_ee_max
REAL*8 Tr,Tdly,dt,t,c,phi,tau,lambda,hbar,m,Pi,z0,vel,dp,KB,Temp,try
REAL*8 CPI,NCPI,Rho_ee_max,Weg,p,mass,Mmntm
COMPLEX*16 Rhogg,Rhoee,Rhoeg,Rhoge,error,Omega,Force
COMPLEX*16 Omegazt,Gamma,Delta,k,F_Num,F_Prev,Omg
COMPLEX*16 Rho_gg_tmp,Rho_ee_tmp,Rho_eg_tmp,Rho_ge_tmp
COMPLEX*16 Rho_gg_error,Rho_ee_error,v,Rho_ee_old
COMPLEX*16 ,PARAMETER :: i = (0,1) ! sqrt(-1)
COMPLEX*16 ,DIMENSION(1:1)::ggk1,ggk2,ggk3,ggk4,ggk5,ggk6
COMPLEX*16 ,DIMENSION(1:1)::eek1,eek2,eek3,eek4,eek5,eek6
COMPLEX*16 ,DIMENSION(1:1)::gek1,gek2,gek3,gek4,gek5,gek6
COMPLEX*16 ,DIMENSION(1:1)::egk1,egk2,egk3,egk4,egk5,egk6
COMPLEX*16 ,DIMENSION(1:1,1:2)::Rho_gg,Rho_ee,Rho_ge,Rho_eg
```

```
DATA Tr,tau,c,lambda,hbar,KB/4.D-9,100D-15,2.998D8,589.D-9/
DATA hbar,KB/1.054571628D-34,1.3806503D-23
DATA e,g/2,1/
DATA va,vb/1,1/
WRITE(*,*)"======================================"
WRITE(*,*)              "Laser cooling of two level atom system"
WRITE(*,*)"======================================"
! open(1,file='Ree.txt')
open(2,file='Force.txt')
open(3,file='dp&d=+G.txt')
! open(4,file='paramers.txt')
!================== initial inputs ==================
! CHANGING TERMS AFTER EACH LOOP
v=(0.0,0.0)
! NOT CHANGING TERMS AFTER EACH LOOP
10 t=0.0; dt=5.D-15; Pi=DAcos(-1.0)
Nr=25.; tstep=1; termn=1;
z0=0.0; p=0.0; Temp=0.0;
Weg=2.*Pi*c/lambda; mass=38.2D-27; F_Num=(0.0,0.0)
Gamma=(62203534.54,0.0); Omega=(10.**0.)*Gamma; Delta=(-2.)*Gamma
k=(0.0,0.0)+2.*Pi/(lambda*Sqrt((1-v/c)/(1+v/c))); vel=Real(v)
Temp=mass*(REAL(v))**2/KB; !v=(0.0,0.0)+Sqrt(KB*Temp/mass)
!================== main loop ==================
Rho_gg(1,1)=(1.0,0.0);Rho_ee(1,1)=(0.0,0.0);Rho_ge(1,1)=(0.0,0.0)
Rho_eg(1,1)=(0.0,0.0)
```

```
1 Loop_1 : Do

Do j=1,va ! Reset the values.
ggk1(j)=(0.0,0.0);ggk2(j)=(0.0,0.0);ggk3(j)=(0.0,0.0)
ggk4(j)=(0.0,0.0);ggk5(j)=(0.0,0.0);ggk6(j)=(0.0,0.0)
gek1(j)=(0.0,0.0);gek2(j)=(0.0,0.0);gek3(j)=(0.0,0.0)
gek4(j)=(0.0,0.0);gek5(j)=(0.0,0.0);gek6(j)=(0.0,0.0)
ENDDO

Do n=1,vb ! Reset the values.
eek1(n)=(0.0,0.0);eek2(n)=(0.0,0.0);eek3(n)=(0.0,0.0)
eek4(n)=(0.0,0.0);eek5(n)=(0.0,0.0);eek6(n)=(0.0,0.0)
egk1(n)=(0.0,0.0);egk2(n)=(0.0,0.0);egk3(n)=(0.0,0.0)
egk4(n)=(0.0,0.0);egk5(n)=(0.0,0.0);egk6(n)=(0.0,0.0)
ENDDO

Omegazt=Omega*Omg(t,z0,v,Tr,tau,Nr)
!————————————————— K1
DO j=1,va ! gek1(j)
Do n=1,vb
gek1(j)=gek1(j)+dt*Rho_ge_tmp(t,Rho_gg(j,tstep),Rho_ee(n,tstep),&
&Rho_ge(j,tstep),Rho_eg(n,tstep),Gamma,Delta,Omegazt,k,v)
ENDDO
ENDDO

DO n=1,vb ! egk1(n)
```

```
Do j=1,va
egk1(n)=egk1(n)+dt*Rho_eg_tmp(t,Rho_gg(j,tstep),Rho_ee(n,tstep),&
&Rho_ge(j,tstep),Rho_eg(n,tstep),Gamma,Delta,Omegazt,k,v)
ENDDO
ENDDO

DO j=1,va ! ggk1(j)
Do n=1,vb
ggk1(j)=ggk1(j)+dt*Rho_gg_tmp(t,Rho_gg(j,tstep),Rho_ee(n,tstep),&
&Rho_ge(j,tstep),Rho_eg(n,tstep),Gamma,Delta,Omegazt,k,v)
ENDDO
ENDDO

DO n=1,vb ! eek1(n)
Do j=1,va
eek1(n)=eek1(n)+dt*Rho_ee_tmp(t,Rho_gg(j,tstep),Rho_ee(n,tstep),&
&Rho_ge(j,tstep),Rho_eg(n,tstep),Gamma,Delta,Omegazt,k,v)
ENDDO
ENDDO
!————————————————— K2
DO j=1,va ! gek2(j)
Do n=1,vb
gek2(j)=gek2(j)+dt*Rho_ge_tmp(t+dt/4.0,Rho_gg(j,tstep)+ggk1(j)/4.0,&
&Rho_ee(n,tstep)+eek1(j)/4.0,Rho_ge(j,tstep)+gek1(j)/4.0,Rho_eg(n,tstep)&
&+egk1(j)/4.0,Gamma,Delta,Omegazt,k,v)
ENDDO
```

```
ENDDO

DO n=1,vb ! egk2(n)
Do j=1,va
egk2(n)=egk2(n)+dt*Rho_eg_tmp(t+dt/4.0,Rho_gg(j,tstep)+ggk1(j)/4.0,&
&Rho_ee(n,tstep)+eek1(j)/4.0,Rho_ge(j,tstep)+gek1(j)/4.0,Rho_eg(n,tstep)&
&+egk1(j)/4.0,Gamma,Delta,Omegazt,k,v)
ENDDO
ENDDO

DO j=1,va ! ggk2(j)
Do n=1,vb
ggk2(j)=ggk2(j)+dt*Rho_gg_tmp(t+dt/4.0,Rho_gg(j,tstep)+ggk1(j)/4.0,&
&Rho_ee(n,tstep)+eek1(j)/4.0,Rho_ge(j,tstep)+gek1(j)/4.0,Rho_eg(n,tstep)&
&+egk1(j)/4.0,Gamma,Delta,Omegazt,k,v)
ENDDO
ENDDO

DO n=1,vb ! eek2(n)
Do j=1,va
eek2(n)=eek2(n)+dt*Rho_ee_tmp(t+dt/4.0,Rho_gg(j,tstep)+ggk1(j)/4.0,&
&Rho_ee(n,tstep)+eek1(j)/4.0,Rho_ge(j,tstep)+gek1(j)/4.0,Rho_eg(n,tstep)&
&+egk1(j)/4.0,Gamma,Delta,Omegazt,k,v)
ENDDO
ENDDO
!———————————————— K3
```

```
DO j=1,va ! gek3(j)
Do n=1,vb
gek3(j)=gek3(j)+dt*Rho_ge_tmp(t+(3.0*dt/8.0),Rho_gg(j,tstep)&
&+(3.0/32.0)*ggk1(j)+(9.0/32.0)*ggk2(j),Rho_ee(n,tstep)&
&+(3.0/32.0)*eek1(n)+(9.0/32.0)*eek2(n),Rho_ge(j,tstep)+(3.0/32.0)&
&*gek1(j)+(9.0/32.0)*gek2(j),Rho_eg(n,tstep)+(3.0/32.0)egk1(n)&
&+(9.0/32.0)*egk2(n),Gamma,Delta,Omegazt,k,v)
ENDDO
ENDDO

DO n=1,vb ! egk3(n) Do j=1,va
egk3(n)=egk3(n)+dt*Rho_eg_tmp(t+(3.0*dt/8.0),Rho_gg(j,tstep)&
&+(3.0/32.0)*ggk1(j)+(9.0/32.0)*ggk2(j),Rho_ee(n,tstep)+(3.0/32.0)&
&*eek1(n)+(9.0/32.0)*eek2(n),Rho_ge(j,tstep)+(3.0/32.0)*gek1(j)+&
&(9.0/32.0)*gek2(j),Rho_eg(n,tstep)+(3.0/32.0)*egk1(n)+(9.0/32.0)&
&*egk2(n),Gamma,Delta,Omegazt,k,v)
ENDDO
ENDDO

DO j=1,va ! ggk3(j)
Do n=1,vb
ggk3(j)=ggk3(j)+dt*Rho_gg_tmp(t+(3.0*dt/8.0),&
&Rho_gg(j,tstep)+(3.0/32.0)*ggk1(j)+&
&(9.0/32.0)*ggk2(j),Rho_ee(n,tstep)+(3.0/32.0)&
&*eek1(n)+(9.0/32.0)*eek2(n),&
&Rho_ge(j,tstep)+(3.0/32.0)*gek1(j)+(9.0/32.0)&
```

```
&*gek2(j),Rho_eg(n,tstep)+(3.0/32.0)&
&*egk1(n)+(9.0/32.0)*egk2(n),Gamma,Delta,Omegazt,k,v)
ENDDO
ENDDO

DO n=1,vb ! eek1(n)
Do j=1,va
eek3(n)=eek3(n)+dt*Rho_ee_tmp(t+(3.0*dt/8.0),&
&Rho_gg(j,tstep)+(3.0/32.0)*ggk1(j)+&
&(9.0/32.0)*ggk2(j),Rho_ee(n,tstep)+(3.0/32.0)*&
&eek1(n)+(9.0/32.0)*eek2(n),&
&Rho_ge(j,tstep)+(3.0/32.0)*gek1(j)+(9.0/32.0)*&
&gek2(j),Rho_eg(n,tstep)+(3.0/32.0)&
&*egk1(n)+(9.0/32.0)*egk2(n),Gamma,Delta,Omegazt,k,v)
ENDDO
ENDDO
!————————————————— K4
DO j=1,va ! gek4(j)
Do n=1,vb
gek4(j)=gek4(j)+dt*Rho_ge_tmp(t+(12.0*dt/13.0),&
&Rho_gg(j,tstep)+(1932.0/2197.0)&
&*ggk1(j)-(7200.0/2197.0)*ggk2(j)+(7296.0/2197.0)&
&*ggk3(j),Rho_ee(n,tstep)+(1932.0/2197.0)&
&*eek1(n)-(7200.0/2197.0)*eek2(n)+(7296.0/2197.0)&
&*eek3(n),Rho_ge(j,tstep)+(1932.0/2197.0)*&
&gek1(j)-(7200.0/2197.0)*gek2(j)+(7296.0/2197.0)&
```

```
&*gek3(j),Rho_eg(n,tstep)+(1932.0/2197.0)*&
&egk1(n)-(7200.0/2197.0)*egk2(n)+(7296.0/2197.0)&
&*egk3(n),Gamma,Delta,Omegazt,k,v)
ENDDO
ENDDO

DO n=1,vb ! egk4(n)
Do j=1,va
egk4(n)=egk4(n)+dt*Rho_eg_tmp(t+(12.0*dt/13.0),&
&Rho_gg(j,tstep)+(1932.0/2197.0)&
&*ggk1(j)-(7200.0/2197.0)*ggk2(j)+(7296.0/2197.0)*&
&ggk3(j),Rho_ee(n,tstep)+(1932.0/2197.0)&
&*eek1(n)-(7200.0/2197.0)*eek2(n)+(7296.0/2197.0)*&
&eek3(n),Rho_ge(j,tstep)+(1932.0/2197.0)*&
&gek1(j)-(7200.0/2197.0)*gek2(j)+(7296.0/2197.0)&
&*gek3(j),Rho_eg(n,tstep)+(1932.0/2197.0)*&
&egk1(n)-(7200.0/2197.0)*egk2(n)+(7296.0/2197.0)&
&*egk3(n),Gamma,Delta,Omegazt,k,v)
ENDDO
ENDDO

DO j=1,va ! ggk4(j)
Do n=1,vb
ggk4(j)=ggk4(j)+dt*Rho_gg_tmp(t+(12.0*dt/13.0),&
&Rho_gg(j,tstep)+(1932.0/2197.0)&
&*ggk1(j)-(7200.0/2197.0)*ggk2(j)+(7296.0/2197.0)&
```

```
&*ggk3(j),Rho_ee(n,tstep)+(1932.0/2197.0)&
&*eek1(n)-(7200.0/2197.0)*eek2(n)+(7296.0/2197.0)&
&*eek3(n),Rho_ge(j,tstep)+(1932.0/2197.0)*&
&gek1(j)-(7200.0/2197.0)*gek2(j)+(7296.0/2197.0)&
&*gek3(j),Rho_eg(n,tstep)+(1932.0/2197.0)*&
&egk1(n)-(7200.0/2197.0)*egk2(n)+(7296.0/2197.0)&
&*egk3(n),Gamma,Delta,Omegazt,k,v)
ENDDO
ENDDO

DO n=1,vb ! eek4(n)
Do j=1,va
eek4(n)=eek4(n)+dt*Rho_ee_tmp(t+(12.0*dt/13.0),&
&Rho_gg(j,tstep)+(1932.0/2197.0)&
&*ggk1(j)-(7200.0/2197.0)*ggk2(j)+(7296.0/2197.0)&
&*ggk3(j),Rho_ee(n,tstep)+(1932.0/2197.0)&
&*eek1(n)-(7200.0/2197.0)*eek2(n)+(7296.0/2197.0)&
&*eek3(n),Rho_ge(j,tstep)+(1932.0/2197.0)*&
&gek1(j)-(7200.0/2197.0)*gek2(j)+(7296.0/2197.0)&
&*gek3(j),Rho_eg(n,tstep)+(1932.0/2197.0)*&
&egk1(n)-(7200.0/2197.0)*egk2(n)+(7296.0/2197.0)&
&*egk3(n),Gamma,Delta,Omegazt,k,v)
ENDDO
ENDDO
!————————————————— K5
```

```
    DO j=1,va ! gek5(j)
Do n=1,vb
gek5(j)=gek5(j)+dt*Rho_ge_tmp(t+dt,Rho_gg(j,tstep)&
&+(439.0/216.0)*ggk1(j)-8.0*ggk2(j)&
&+(3680.0/513.0)*ggk3(j)-(845.0/4104.0)*ggk4(j),&
&Rho_ee(n,tstep)+(439.0/216.0)*eek1(n)&
&-8.0*eek2(n)+(3680.0/513.0)*eek3(n)-(845.0/4104.0)&
&*eek4(n),Rho_ge(j,tstep)+(439.0/216.0)&
&*gek1(j)-8.0*gek2(j)+(3680.0/513.0)*gek3(j)-&
&(845.0/4104.0)*gek4(j),Rho_eg(n,tstep)&
&+(439.0/216.0)*egk1(n)-8.0*egk2(n)+(3680.0/513.0)&
&*egk3(n)-(845.0/4104.0)*egk4(n)&
&,Gamma,Delta,Omegazt,k,v)
ENDDO
ENDDO

DO n=1,vb ! egk5(n)
Do j=1,va
egk5(n)=egk5(n)+dt*Rho_eg_tmp(t+dt,Rho_gg(j,tstep)&
&+(439.0/216.0)*ggk1(j)-8.0*ggk2(j)&
&+(3680.0/513.0)*ggk3(j)-(845.0/4104.0)*ggk4(j),&
&Rho_ee(n,tstep)+(439.0/216.0)*eek1(n)&
&-8.0*eek2(n)+(3680.0/513.0)*eek3(n)-(845.0/4104.0)&
&*eek4(n),Rho_ge(j,tstep)+(439.0/216.0)&
&*gek1(j)-8.0*gek2(j)+(3680.0/513.0)*gek3(j)-&
&(845.0/4104.0)*gek4(j),Rho_eg(n,tstep)&
```

```
&+(439.0/216.0)*egk1(n)-8.0*egk2(n)+(3680.0/513.0)&
&*egk3(n)-(845.0/4104.0)*egk4(n)&
&,Gamma,Delta,Omegazt,k,v)
ENDDO
ENDDO

DO j=1,va ! ggk5(j)
Do n=1,vb
ggk5(j)=ggk5(j)+dt*Rho_gg_tmp(t+dt,Rho_gg(j,tstep)&
&+(439.0/216.0)*ggk1(j)-8.0*ggk2(j)&
&+(3680.0/513.0)*ggk3(j)-(845.0/4104.0)*ggk4(j),&
&Rho_ee(n,tstep)+(439.0/216.0)*eek1(n)&
&-8.0*eek2(n)+(3680.0/513.0)*eek3(n)-(845.0/4104.0)&
&*eek4(n),Rho_ge(j,tstep)+(439.0/216.0)&
&*gek1(j)-8.0*gek2(j)+(3680.0/513.0)*gek3(j)-&
&(845.0/4104.0)*gek4(j),Rho_eg(n,tstep)&
&+(439.0/216.0)*egk1(n)-8.0*egk2(n)+(3680.0/513.0)&
&*egk3(n)-(845.0/4104.0)*egk4(n)&
&,Gamma,Delta,Omegazt,k,v)
ENDDO
ENDDO

DO n=1,vb ! eek5(n)
Do j=1,va
eek5(n)=eek5(n)+dt*Rho_ee_tmp(t+dt,Rho_gg(j,tstep)&
&+(439.0/216.0)*ggk1(j)-8.0*ggk2(j)&
```

```
&+(3680.0/513.0)*ggk3(j)-(845.0/4104.0)*ggk4(j),&
&Rho_ee(n,tstep)+(439.0/216.0)*eek1(n)&
&-8.0*eek2(n)+(3680.0/513.0)*eek3(n)-(845.0/4104.0)&
&*eek4(n),Rho_ge(j,tstep)+(439.0/216.0)&
&*gek1(j)-8.0*gek2(j)+(3680.0/513.0)*gek3(j)-&
&(845.0/4104.0)*gek4(j),Rho_eg(n,tstep)&
&+(439.0/216.0)*egk1(n)-8.0*egk2(n)+(3680.0/513.0)&
&*egk3(n)-(845.0/4104.0)*egk4(n)&
&,Gamma,Delta,Omegazt,k,v)
ENDDO
ENDDO
!————————————————— K6
DO j=1,va ! gek6(j)
Do n=1,vb
gek6(j)=gek6(j)+dt*Rho_ge_tmp(t+dt/2.0,&
&Rho_gg(j,tstep)-(8.0/27.0)*ggk1(j)+2.0*ggk2(j)&
&-(3544.0/2565.0)*ggk3(j)+(1859.0/4104.0)*ggk4(j)&
&-(11.0/40.0)*ggk5(j),Rho_ee(n,tstep)&
&-(8.0/27.0)*eek1(n)+2.0*eek2(n)-(3544.0/2565.0)&
&*eek3(n)+(1859.0/4104.0)*eek4(n)-&
&(11.0/40.0)*eek5(n),Rho_ge(j,tstep)-(8.0/27.0)&
&*gek1(j)+2.0*gek2(j)-(3544.0/2565.0)&
&*gek3(j)+(1859.0/4104.0)*gek4(j)-(11.0/40.0)&
&*gek5(j),Rho_eg(n,tstep)-(8.0/27.0)*&
&egk1(n)+2.0*egk2(n)-(3544.0/2565.0)*egk3(n)&
&+(1859.0/4104.0)*egk4(n)-(11.0/40.0)*&
```

```
&egk5(n),Gamma,Delta,Omegazt,k,v)
ENDDO
ENDDO

DO n=1,vb ! egk6(n) Do j=1,va
egk6(n)=egk6(n)+dt*Rho_eg_tmp(t+dt/2.0,&
&Rho_gg(j,tstep)-(8.0/27.0)*ggk1(j)+2.0*ggk2(j)&
&-(3544.0/2565.0)*ggk3(j)+(1859.0/4104.0)*ggk4(j)&
&-(11.0/40.0)*ggk5(j),Rho_ee(n,tstep)&
&-(8.0/27.0)*eek1(n)+2.0*eek2(n)-(3544.0/2565.0)&
&*eek3(n)+(1859.0/4104.0)*eek4(n)-&
&(11.0/40.0)*eek5(n),Rho_ge(j,tstep)-(8.0/27.0)&
&*gek1(j)+2.0*gek2(j)-(3544.0/2565.0)&
&*gek3(j)+(1859.0/4104.0)*gek4(j)-(11.0/40.0)*&
&gek5(j),Rho_eg(n,tstep)-(8.0/27.0)*&
&egk1(n)+2.0*egk2(n)-(3544.0/2565.0)*egk3(n)+&
&(1859.0/4104.0)*egk4(n)-(11.0/40.0)*&
&egk5(n),Gamma,Delta,Omegazt,k,v)
ENDDO
ENDDO

DO j=1,va ! ggk6(j)
Do n=1,vb
ggk6(j)=ggk6(j)+dt*Rho_gg_tmp(t+dt/2.0,&
&Rho_gg(j,tstep)-(8.0/27.0)*ggk1(j)+2.0*ggk2(j)&
&-(3544.0/2565.0)*ggk3(j)+(1859.0/4104.0)*ggk4(j)&
```

```
&-(11.0/40.0)*ggk5(j),Rho_ee(n,tstep)&
&-(8.0/27.0)*eek1(n)+2.0*eek2(n)-(3544.0/2565.0)&
&*eek3(n)+(1859.0/4104.0)*eek4(n)-&
&(11.0/40.0)*eek5(n),Rho_ge(j,tstep)-(8.0/27.0)&
&*gek1(j)+2.0*gek2(j)-(3544.0/2565.0)&
&*gek3(j)+(1859.0/4104.0)*gek4(j)-(11.0/40.0)&
&*gek5(j),Rho_eg(n,tstep)-(8.0/27.0)*&
&egk1(n)+2.0*egk2(n)-(3544.0/2565.0)*egk3(n)&
&+(1859.0/4104.0)*egk4(n)-(11.0/40.0)*&
&egk5(n),Gamma,Delta,Omegazt,k,v)
ENDDO
ENDDO

DO n=1,vb ! eek6(n)
Do j=1,va
eek6(n)=eek6(n)+dt*Rho_ee_tmp(t+dt/2.0,Rho_gg(j,tstep)&
&-(8.0/27.0)*ggk1(j)+2.0*ggk2(j)&
&-(3544.0/2565.0)*ggk3(j)+(1859.0/4104.0)*ggk4(j)&
&-(11.0/40.0)*ggk5(j),Rho_ee(n,tstep)&
&-(8.0/27.0)*eek1(n)+2.0*eek2(n)-(3544.0/2565.0)&
&*eek3(n)+(1859.0/4104.0)*eek4(n)-&
&(11.0/40.0)*eek5(n),Rho_ge(j,tstep)-(8.0/27.0)&
&*gek1(j)+2.0*gek2(j)-(3544.0/2565.0)&
&*gek3(j)+(1859.0/4104.0)*gek4(j)-(11.0/40.0)&
&*gek5(j),Rho_eg(n,tstep)-(8.0/27.0)*&
&egk1(n)+2.0*egk2(n)-(3544.0/2565.0)*egk3(n)&
```

```
&+(1859.0/4104.0)*egk4(n)-(11.0/40.0)*&
&egk5(n),Gamma,Delta,Omegazt,k,v)
ENDDO
ENDDO
Do j=1,va
Rho_ge(j,tstep+1)=Rho_ge(j,tstep)+(16.0/135.0)*gek1(j)+(0.0)&
&*gek2(j)+(6656.0/12825.0)*gek3(j)+(28561.0/56430.0)*gek4(j)*gek2(j)&
&+(6656.0/12825.0)-(9.0/50.0)*gek5(j)+(2.0/55.0)*gek6(j)
Rho_gg(j,tstep+1)=Rho_gg(j,tstep)+(16.0/135.0)*ggk1(j)+(0.0)&
&*ggk2(j)+(6656.0/12825.0)*ggk3(j)+(28561.0/56430.0)*ggk4(j)
-(9.0/50.0)*ggk5(j)+(2.0/55.0)*ggk6(j)
Rho_gg_error=(1.0/360.0)*ggk1(j)-(128.0/4275.0)*ggk3(j)&
&-(2197.0/75240.0)*ggk4(j)+(1.0/50.0)*ggk5(j)+(2.0/55.0)*ggk6(j)

Rho_ge(j,tstep)=Rho_ge(j,tstep+1)
Rho_gg(j,tstep)=Rho_gg(j,tstep+1)

ENDDO

Do n=1,vb
Rho_eg(n,tstep+1)=Rho_eg(n,tstep)+(16.0/135.0)*egk1(n)+&
&(0.0)*egk2(n)+(6656.0/12825.0)*egk3(n)+(28561.0/56430.0)
*egk4(n)-(9.0/50.0)*egk5(n)+(2.0/55.0)*egk6(n)
Rho_ee(n,tstep+1)=Rho_ee(n,tstep)+(16.0/135.0)*eek1(n)&
&+(0.0)*eek2(n)+(6656.0/12825.0)*eek3(n)+(28561.0/56430.0)
*eek4(n)-(9.0/50.0)*eek5(n)+(2.0/55.0)*eek6(n)
```

```
Rho_ee_error=(1.0/360.0)*eek1(n)-(128.0/4275.0)&
&*eek3(n)-(2197.0/75240.0)*eek4(n)+(1.0/50.0)*eek5(n)
+(2.0/55.0)*eek6(n)
!========== Population of the excited state ============
! If(Mod(termn,100).EQ.0.0) Then
! Write(1,*)t,Real(Omegazt)!Real(Rho_ee(n,tstep))
! Write(1,*)t,Real(Rho_ee(n,tstep))
! Else
! ENDIF
Rho_ee_old=Real(Rho_ee(n,tstep))
Rho_eg(n,tstep)=Rho_eg(n,tstep+1)
Rho_ee(n,tstep)=Rho_ee(n,tstep+1)
ENDDO
!================== Force & Momentum ==================
F_prev=F_Num
F_Num=-Force(t,z0,v,Tr,tau,k,Omegazt,Rho_eg(n,tstep),Delta,Nr)
P=P+0.5*dt*(Real(F_Num)+Real(F_prev))
!================== Error correction ==================
If(Real(Rho_ee_error).GE.10.**-14.)Then
dt=dt/2.
Else
IF(dt.LE.tau/5.)Then
dt=dt*2.
ELSE
ENDIF
ENDIF
```

```
t=t+dt; termn=termn+1
If (t.GT.(Nr+0.2)*Tr) Exit Loop_1
END DO Loop_1
Write(2,*)REAL(k*v/Gamma),Real(F_Num/(k*hbar*Gamma)),Aimag(Rho_eg(n,tstep))
! Write(*,*)REAL(k*v/Gamma),Real(F_Num/(k*hbar*Gamma)),Aimag(Rho_eg(n,tstep))
write(3,*)(REAL(k)*REAL(v)),p/(hbar*Real(k))
! write(*,*)(REAL(k)*REAL(v))/(250000000.*2.*Pi),p/(hbar*Real(k))
If (REAL(v).LT.50.)then
v=v+(2.,0.0)
GOTO 10
ELSE
ENDIF
!================== parameters ===================
Write(*,*)"Rabi's frequency =",Real(Omega)," Hz"
Write(*,*)"Radiating rate =",Real(Gamma)," Photon per sec"
Write(*,*)"Ratio of Omega to Gamma =",Nint(Real(Omega)/Real(Gamma))
Write(*,*)"Life time =",(1./Real(Gamma))/1.D-9," nsec"
Write(*,*)"Resonance frequency =",Weg ,"Hz"
Write(*,*)"detuning =",Real(Delta) ,"Hz"
Write(*,*)"Effective detuning =",Real(Delta)-Real(k)*real(v) ,"Hz"
Write(*,*)"wave number k =",Real(k) ,"m^-1"
2 Close(1);Close(2);Close(3)
Stop
END
!================== Functions ===================
FUNCTION Rho_gg_tmp(t,Rhogg,Rhoee,Rhoge,Rhoeg,Gamma,Delta,Omegazt,k,v)
```

```
REAL*8 t
Complex*16 Rho_gg_tmp,Rhogg,Rhoee,Rhoge,Rhoeg,Gamma,Delta,Omegazt
COMPLEX*16, PARAMETER :: i = (0,1) ! sqrt(-1)
Rho_gg_tmp=+Gamma*Rhoee+i/2.0*(Conjg(Omegazt)*Rhoeg-Omegazt*Rhoge)
End FUNCTION Rho_gg_tmp

FUNCTION Rho_ee_tmp(t,Rhogg,Rhoee,Rhoge,Rhoeg,Gamma,Delta,Omegazt,k,v)
REAL*8 t
Complex*16 Rho_ee_tmp,Rhogg,Rhoee,Rhoge,Rhoeg,Gamma,Delta,Omegazt
COMPLEX*16, PARAMETER :: i = (0,1) ! sqrt(-1)
Rho_ee_tmp=-Gamma*Rhoee+i/2.0*(Omegazt*Rhoge-Conjg(Omegazt)*Rhoeg)
End FUNCTION Rho_ee_tmp

FUNCTION Rho_ge_tmp(t,Rhogg,Rhoee,Rhoge,Rhoeg,Gamma,Delta,Omegazt,k,v)
REAL*8 t
Complex*16 Rho_ge_tmp,Rhogg,Rhoee,Rhoge,Rhoeg,Gamma,Delta,Omegazt,k,v
COMPLEX*16, PARAMETER :: i = (0,1) ! sqrt(-1)
Rho_ge_tmp=-(Gamma/2.0+i*(Delta+k*v))*Rhoge+i/2.0*Conjg(Omegazt)*(Rhoee-
Rhogg)
End FUNCTION Rho_ge_tmp

FUNCTION Rho_eg_tmp(t,Rhogg,Rhoee,Rhoge,Rhoeg,Gamma,Delta,Omegazt,k,v)
REAL*8 t
Complex*16 Rho_eg_tmp,Rhogg,Rhoee,Rhoge,Rhoeg,Gamma,Delta,Omegazt,k,v
COMPLEX*16, PARAMETER :: i = (0,1) ! sqrt(-1)
Rho_eg_tmp=-(Gamma/2.0-i*(Delta+k*v))*Rhoeg+i/2.0*Omegazt*(Rhogg-Rhoee)
```

```
End FUNCTION Rho_eg_tmp

Function Omg(t,z0,v,Tr,tau,Nr)
Integer*8 Nr,m
REAL*8 t,tau,Tr,z,z0,c
Complex*16 Omg,v
Data c/2.998D8/
Omg=(0.0,0.0)
z=z0+Real(v)*t
Omg=(0.0,0.0)
Do m=1,Nr
Omg=Omg+Exp(-(t+(z/c)-m*Tr)**2./(2.*tau**2.))
ENDD
End FUNCTION Omg

Function Force(t,z0,v,Tr,tau,k,Omegazt,Rhoegtmp,Delta,Nr) ! f(t)
Integer*8 Nr,m
Real*8 c,t,z,z0,Tr,tau
COMPLEX*16, PARAMETER :: i = (0,1) ! sqrt(-1)
COMPLEX*16 k,hbar,Rhoegtmp,Omegazt,Force,v
z=z0+Real(v)*t
hbar=(1.054571628D-34,0.0)
Force=i*k*hbar*(Omegazt*Conjg(Rhoegtmp)-Conjg(Omegazt)*Rhoegtmp)
End FUNCTION Force
```